

**SYNTHESIS AND CHARACTERIZATION OF  
BORON COMPOSITE NANOPARTICLES FOR  
WEAR AND FRICTION REDUCTION**

**A Thesis Submitted to  
the Graduate School of Engineering and Sciences of  
İzmir Institute of Technology  
in Partial Fulfillments of the Requirements for the Degree of**

**MASTER OF SCIENCE**

**in Chemical Engineering**

**by  
Esin GÖKMEN**

**July 2019  
İZMİR**

We approve the thesis of **Esin GÖKMEN**

**Examining Committee Members:**

---

**Prof. Dr. Mehmet POLAT**

Department of Chemical Engineering, İzmir Institute of Technology

---

**Prof. Dr. Ekrem ÖZDEMİR**

Department of Chemical Engineering, İzmir Institute of Technology

---

**Prof. Dr. Mustafa DEMİRCİOĞLU**

Department of Chemical Engineering, Ege University

**12 July 2019**

---

**Prof. Dr. Mehmet POLAT**

Supervisor, Department of Chemical Engineering  
İzmir Institute of Technology

---

**Prof. Dr. Erol ŞEKER**

Head of the Department of Chemical  
Engineering

---

**Prof. Dr. Aysun SOFUOĞLU**

Dean of the Graduate School of  
Engineering and Sciences

## ACKNOWLEDGMENTS

Foremost, I would like to express my very great appreciation to my advisor **Prof. Dr. Mehmet POLAT** for his valuable and constructive suggestions, continuous support during the planning and development of this research work. I could not have imagined having better mentor for my study.

I would like to offer my special thanks to my co-advisor **Prof. Dr. Hürriyet POLAT**. Her guidance helped me in all time of research and writing of this thesis. Her willingness to give his time so generously has been very much appreciated.

I wish to thank to **Prof. Dr. Mustafa DEMİRCİOĞLU** and **Prof. Dr. Ekrem ÖZDEMİR** for accepting to be part of the Thesis Defense Jury.

My special thanks are extended to the **R&D staff of Opet Fuchs** for their valuable support.

I am thankful to my lab-mate **Elif Suna SOP** for their endless supports and contributions during my experiments. I feel very lucky to know her and to be her friend.

I would like to express my gratitude to my dear friends **Ayşe METECAN, Aydın CİHANOĞLU, Merve DEMİRKURT, Ece Zeynep TÜZÜN, Gizem CİHANOĞLU** and **Önder TEKİNALP** for their patience and support during writing of my thesis.

Finally, and the most important, I am really indebted to my family, my sister **Emel DURAN** and my dream partner **Ulaş ATIKLER** for giving me chance to improve myself, and also their unconditional love, endless courage and precious support.

## ABSTRACT

### SYNTHESIS AND CHARACTERIZATION OF BORON COMPOSITE NANOPARTICLES FOR WEAR AND FRICTION REDUCTION

Since most of the conventional lubricants reach their performance limits, new antiwear and extreme pressure (EP) additives are designed so that lubricants can minimize friction and wear when used in high temperature and pressure conditions. There is growing interest in the use of nanoparticles as an additive in lubricants. Due to its outstanding chemical properties, boron is frequently involved in the design of nanoparticles. Especially borate derivatives and hexagonal boron nitride (h-BN) have already taken their places in many lubricant formulations.

The aim of this study was the production of silica-boron composite nanoparticles that can replace the phosphate-derived additives used in lubricant formulations and to provide the extreme pressure, antiwear and friction-regulating properties at the same time. For this purpose, the Stöber method that is used for silica production was modified to produce Si/Na-Borate nanoparticles. It was found that the synthesis of composite nanoparticles in desired size distribution and morphology as well as composite structures composed of Si and Na-Borate, was possible changing the amounts of ingredients and modes of addition. It was observed that the morphology and the chemical structure of these particles depend on the amount of Na-Borate (1, 3, and 5% w/w) and the addition type of Na-Borate (Direct, 500  $\mu\text{L}/\text{min}$ , 5 $\mu\text{L}/\text{min}$ ). Then composite nanoparticles were characterized using SEM, FTIR and ICP-MS and some tests were conducted to examine the structure of particles.

The tribological performance of these particles tested using Four Ball Test method have shown that there is a significant improvement in the presence of these particles.

## ÖZET

### AŞINMA VE SÜRTÜNMEYİ AZALTMAK İÇİN BOR KOMPOZİT NANOTANELERİN SENTEZİ VE KARAKTERİZASYONU

Konvansiyonel olarak kullanılan yağlayıcıların çoğu performans sınırlarına ulaştığı için yağlayıcıların yüksek sıcaklık ve basınç koşullarında kullanıldığında sürtünme ve aşınmayı minimize edebilmeleri amacıyla yeni aşınma önleyici (AW: Antiwear) ve aşırı basınç (EP: Extreme Pressure) katkıları tasarlanmaktadır. Nanotanelerin yağlayıcılarda katkı olarak kullanımını konusunda giderek artan bir ilgi vardır. Öne çıkan kimyasal özellikleri nedeniyle bor, nanotanelerin tasarımında sıklıkla kullanılmaktadır. Özellikle borat türevleri ve hegzagonal bor nitrür (h-BN) halihazırda bir çok yağlayıcı formülünde yerini almıştır.

Yağlayıcı formülasyonlarında kullanılan fosfat türevli katkıları ikame edebilecek, aşırı basınç koşullarında kullanılacak, aşınma ve sürtünme önleyici özelliklerini aynı anda sağlayabilecek borlu nanotanelerin üretimi ve yeni nesil yağlayıcılarda kullanılması bu tezin en önemli motivasyonudur. Bu amaçla, silika nanotanelerin üretilmesinde kullanılan Stöber yöntemi modifiye edilerek Si/Na-Borate nanotaneleri sentezlenmiştir. Kompozit nanotanelerin istenilen boyut dağılımında ve morfolojisinde sentezlenmesinin, bileşenlerin miktarlarının ve sisteme ilave edilme şeklinin değiştirilmesi ile mümkün olduğu görülmüştür. Kompozit nanotanelerin morfolojisi ve kimyasal yapısının sodyum borat (Na-Borat) çözeltisinin konsantrasyonu (kütlece % 1, 3 ve 5) ve sisteme eklenme şekli ile (bir defada, 500 µL /dk., 5 µL /dk) doğrudan ilişkili olduğu gözlemlenmiştir. Sentezlenen kompozit nanotaneler SEM, FTIR ve ICP-MS kullanılarak karakterize edilmiş ve tanelerin yapısını incelemek için ilave testler de gerçekleştirilmiştir.

Ayrıca sentezlenen nanotanelerin tribolojik performansı, Dört Bilya Test yöntemi kullanılarak test edilmiştir ve tanelerin yağlayıcıların tribolojik özelliklerini geliştirdiği görülmüştür.

# TABLE OF CONTENTS

ACKNOWLEDGMENTS .....	iii
ABSTRACT.....	iv
ÖZET .....	v
TABLE OF CONTENTS.....	vi
LIST OF FIGURES .....	ix
LIST OF TABLES.....	xi
LIST OF ABBREVIATIONS.....	xii
CHAPTER 1. INTRODUCTION .....	1
1.1. Statement of the Problem .....	1
1.2. State of the Art .....	2
1.3. Scope of the Study.....	4
CHAPTER 2. BACKGROUND AND LITERATURE REVIEW .....	5
2.1. Background Information.....	5
2.1.1. Friction .....	5
2.1.2. Wear .....	8
2.1.3. Fundamentals of Lubrication and Lubricants.....	9
2.1.4. Lubrication Regimes and Stribeck Diagram .....	10
2.1.5. Lubricants.....	12
2.1.6. Lubricant Additives.....	13
2.1.7 Antiwear (AW) and Extreme Pressure (EP) Additives.....	18
2.2. Literature Review .....	20
2.2.1 Conventional AW and EP Additives.....	21
2.2.2. Novel AW and EP Additives-Nanoparticles in Lubricants.....	24
2.2.3. Boron Compounds as AW and EP Additives.....	28

CHAPTER 3. MATERIALS AND METHODS .....	36
3.1. Materials .....	36
3.2. Methods .....	36
3.2.1. Synthesis and Characterization of Composite (Si/Na-Borate) Nanoparticles .....	37
3.2.1.1. Effect of Na-Borate Concentration on Synthesis of Composite (Si/Na-Borate) Nanoparticles.....	40
3.2.1.2. Effect of TEOS amount on Synthesis of Composite (Si/Na-Borate) Nanoparticles.....	40
3.2.1.3. Effect of Mode of Na-Borate Addition on Synthesis of Composite (Si/Na-Borate) Nanoparticles .....	41
3.2.1.4. Understanding the Structure of the Composite Nanoparticles.....	41
3.2.1.5. Material Balance .....	42
3.2.2. Tribological Performance of Composite Nanoparticles .....	42
3.2.2.1 Dispersion of Composite Nanoparticles .....	42
3.2.2.2 Four Ball Extreme Pressure Test to define the Load- Wear Index and Weld Point.....	43
CHAPTER 4. RESULTS and DISCUSSIONS .....	46
4.1. Synthesis and Characterization of Composite (Si/Na-Borate) Nanoparticles.....	46
4.1.1. Effect of Na-Borate Concentration on Synthesis of Composite (Si/Na-Borate) Nanoparticles .....	49
4.1.2. Effect of Na-Borate Concentration on the Chemical Structure of Composite Nanoparticles.....	50
4.1.3. Effect of TEOS Concentration on the Chemical Structure of Composite Nanoparticles .....	56
4.1.4. Effect of Mode of Na-Borate Addition on Synthesis of Composite (Si/Na-Borate) Nanoparticles .....	56

4.1.5. Understanding the Structure of the Composite Nanoparticles .	59
4.1.6. Material Balance .....	62
4.2. Tribological Performance of Composite Nanoparticles .....	65
4.2.1. Dispersion of Composite Nanoparticles in Different Medium	65
4.2.2. Four Ball Extreme Pressure Test and Define the Load-Wear Index and Weld Point .....	66
CHAPTER 5. CONCLUSION .....	68
REFERENCES .....	70



## LIST OF FIGURES

<b><u>Figure</u></b>	<b><u>Page</u></b>
Figure 1 Structure of the tribo-system .....	6
Figure 2 Coefficient of friction .....	6
Figure 3 Kinetic Friction vs. Static Friction .....	6
Figure 4 Sliding and rolling .....	7
Figure 5 Engineering description of stick-slip .....	7
Figure 6 Types of wear .....	8
Figure 7 Functions of lubrication additives .....	10
Figure 8 Stribeck diagram represents lubrication regimes .....	11
Figure 9 Tribofilm formation on metal surfaces .....	18
Figure 10 Tribochemical attractions of sulfur additives under extreme conditions .....	21
Figure 11 Structure of ZDDP .....	22
Figure 12 The effect of the alkyl structure on the properties of ZDDP .....	23
Figure 13 Structure of ZDDP tribofilm on metal surface .....	23
Figure 14 Statistics of nanoparticles worked as lubricant additives .....	27
Figure 15 Number of articles in Web of Science .....	30
Figure 16 Structure of boric acid .....	33
Figure 17 Structure of h-BN .....	33
Figure 18 Sketch of the hybrid SiO <sub>2</sub> NPs functionalization .....	34
Figure 19 Schematic diagram of the lubrication mechanism of silica nanoparticle .....	34
Figure 20 Silica network production through the hydrolysis and condensation reactions of TEOS .....	38
Figure 21 Composite (Si/Na-Borate) Silica Synthesis .....	39
Figure 22 Solubility of Na-Borate in water at different temperatures .....	40
Figure 23 Four Ball Tester .....	44
Figure 24 Rotated steel balls in the Four Ball Tester .....	44
Figure 25 Welded balls (left), abrasions on the surface of the ball (right) .....	45
Figure 26 Zeta potential measurements of pure silica and Na-Borate .....	47
Figure 27 Progress of forming composite Silica/Na-Borate nanoparticles .....	48
Figure 28 Difference between Si/Na-Borate composite nanoparticles and pure silica nanoparticles .....	50

<b><u>Figure</u></b>	<b><u>Page</u></b>
Figure 29 SEM pictures of composite nanoparticles contain 1 to 10% Na-Borate in comparison with neat silica particles .....	51
Figure 30 XRD results of composite nanoparticles .....	52
Figure 31 FTIR analysis result of composite nanoparticle with 1% Na-Borate .....	53
Figure 32 FTIR analysis result of composite nanoparticle with 3% Na-Borate .....	54
Figure 33 FTIR analysis result of composite nanoparticle with 5% Na-Borate .....	54
Figure 34 FTIR analysis result of composite nanoparticle with 9% Na-Borate .....	55
Figure 35 SEM pictures of nanoparticles contain 1%, 3% and 5% Na-Borate, effect of TEOS amount .....	57
Figure 36 SEM pictures of nanoparticles that contain 5% Na-Borate synthesized with addition rate of direct, 500 $\mu$ L/min and 50 $\mu$ L/min. ....	58
Figure 37 SEM pictures and size distributions of nanoparticles that contain 5% Na-Borate synthesized for repeatability test. ....	59
Figure 38 Effect of simple washing on morphology of composite nanoparticles. ....	60
Figure 39 Borate ions at different pH levels .....	61
Figure 40 Literature example of precipitate structure .....	61
Figure 41 Literature example of easily removed cementing structure .....	62
Figure 42 FTIR results of before and after treatment with water. ....	64
Figure 43 XRD results of before and after treatment with water. ....	64
Figure 44 Mechanism of forming composite structure .....	65
Figure 45 Stability results of composite nanoparticles dispersed in base oil. ....	66

## LIST OF TABLES

<b><u>Table</u></b>	<b><u>Page</u></b>
Table 1 Base oil groups and characteristics.....	12
Table 2 Surface tension of several base oils.....	13
Table 3 Common properties of base oils.....	15
Table 4 Properties of different synthetic base oils.....	16
Table 5 Differences of EP and AW additives.....	19
Table 6 Summary of nano-sized lubricant additives.....	26
Table 7 Types of nanoparticles as lubricant additives.....	26
Table 8 Summary of reported effects of nanoparticles on tribological properties.....	29
Table 9 Literature review of borate nanoparticles.....	31
Table 10 ICP-MS results of composite nanoparticles.....	52
Table 11 ICP-MS results of simple washing test.....	60
Table 12 ICP results of supernatant.....	63
Table 13 ICP results of solid part.....	63
Table 14 Four Ball Test - EP performance results of composite nanoparticles.....	67

## LIST OF ABBREVIATIONS

AW: Antiwear

CTAB: Cetyl Trimethyl Ammonium Bromide

DBDS: Dibenzyl Disulfide

DLS: Dynamic Light Scattering

DMTD: 2,5-dimercapto-1,3,4-thiadiazole

EP: Extreme Pressure

FeB, Fe<sub>2</sub>B: Ferric Boride

FTIR: Fourier Transform Infrared Spectrophotometer

h-BN: Hexagonal Boron Nitride

ICP-MS: Inductively Coupled Plasma Mass Spectrometry

MBT: 2-mercapto-1,3-benzothiazole

Na-Borate: di-Sodium Tetraborate Decahydrate

NH<sub>4</sub>OH: Ammonium Hydroxide

PTFE: Polytetrafluoroethylene

SEM: Scanning Electron Microscopy

TCP: Tricresyl Phosphate

TEOS: Tetraethyl Orthosilicate

ZDDP: Zinc Dialkyl Dithiophosphate

# CHAPTER 1

## INTRODUCTION

Machine designs have been continually improved to enhance performance, increase efficiency, and at the same time meet environmental regulations. Lubricants that cover moving parts and protect components of machines are an essential contributor to reliability and durability of modern machine elements. Preservation of a lubricating film between moving parts is a vital function. Lubricants must prevent metal-to-metal contact that will result in wear. Full-film lubrication occurs when moving surfaces are continuously separated by a film of lubricant. When machines heat up, thickness of a lubricant film has to stay between specified limits to be able to provide adequate lubrication. Viscosity of lubricant is a measure to specify these limits. Contrarily, lubricants act as a coolant. Rust and corrosion protection of a wide range of machine parts is also provided by the use lubricants.

Modern lubricants should be formulated with latest friction or viscosity modifying properties. This is to enable reduction of friction between moving surfaces and providing favorable improved viscosity profiles that lead to higher thermal efficiency. Frequently machine designers reach chemical or physical limits that they can only overcome when they are supported by increased performance from lubricant formulations. Lubricants are in many cases no longer only a commodity but rather an important design element of new machine development programs. Research is ongoing to formulate lubricants to meet the demands of latest machine designs. Beside their main task modern lubricants must perform several additional functions to cover the needs of modern machines.

### 1.1. Statement of the Problem

In order for any machine to operate evenly, it is necessary to provide the energy corresponding to the frictional force. Efficiency of the machines can be upgraded by reduce energy lost caused by friction. Friction losses have an enormous effect on national

economies due to loss of machine components and maintenance costs to avoid wear. Recent studies have shown that in three main areas, power generation, transport and industrial processes, 11 % of total annual energy losses can be saved by developments in lubricant technology.<sup>1</sup>

Thus, with the existing lubricants reaching their performance limits, one of the greatest scientific challenges of the 21st century is to develop new lubricants that meet the requirements when used under harsh conditions. Searching for different ways to save energy opened new research area for developing novel materials instead of traditional one that use as lubricant additives.

For this reason, new technologies have been started to be used for producing lubricant additives. Over the past few years, the biggest development in lubrication has been adaptation of nanotechnology to additive synthesis. A significant decrease in friction coefficients was recorded with using nanoparticles as lubricant additives.

## **1.2. State of the Art**

Lubricants mainly consist of three different components. These are base oils, surface additives and other additives including antiwear (AW) and extreme pressure (EP) additives. There are many reasons for using nanoparticles in lubricant formulations. Some of them are listed below.

- They are easily contact the moving surfaces due their small size
- They do not clog up oil filters thanks to their small size
- They have lower probability of interacting with other lubricant additives
- They have high film formation potentials on different types of surfaces
- They are also highly durable
- At high temperature levels, they show low-volatility behavior.

The main function of lubricant additives is to increase the lubrication properties and to protect the components that are exposed to high temperature and pressure. Many additives used in lubricant formulations include chlorine, sulfur and phosphorus

compounds. Their use is restricted due to environmental hazards. In recent years, the design of environmentally friendly additives, which can partially or totally replace the Zinc Dialkyl Dithiophosphate (ZDDP) contribution, has gained importance. For this purpose, the use of nanotechnology has become increasingly important due to the extended physical and chemical properties. Instead of chlorine, sulfur and phosphorus compounds, borate compounds have been used by result of their low environmental effects and high wear resistance performance.

Researchers have focused on studies of boric acid as a lubricant additive among other boron compounds. With using boric acid as a lubricant additive, the coefficient of friction on metal and ceramic surfaces was decreased. Otherwise, nano-sized boric acid could be used with many additives properly. However, when the nano-boric acid is exposed to water in particular, the tendency to agglomeration makes it difficult to increase the particle size and to disperse in the base oil. Surfactant can be used to solve this problem. However, characteristics of lubricants can partially or completely change by using surfactant even at small amounts. Hence, the actual solution is that the boron-based additives are designed to be easily dispersed during the synthesis phase. Also, they can be modified after production.

There are many different studies in the literature regarding usage of boron derivatives as lubricant additives in recent years. There is an increasing interest in borate-based materials in the field of tribology. For example;

- Calcium borate,<sup>2-4</sup>
- Lanthanum borate,<sup>5</sup>
- Magnesium borate<sup>6</sup> and aluminum borate,<sup>7</sup>
- Zinc borate,<sup>8</sup>
- Potassium borate<sup>9</sup>
- Cerium borate<sup>10</sup> are used as AW and EP additives in the literature.

In the light of these studies, we can conclude that borate derivatives improve the wear resistance and reduce the friction. It is observed that, nanoparticles used as potential lubricant additives in different structure and morphology. Many experiments have been carried out by researchers as of today, but very few of the nanoparticles have been commercialized and their tribological behavior has been fully understood. Lastly but most

importantly, usage of composite nanoparticles contain silica and borate derivatives as lubricant additives have not been found in literature.

### **1.3. Scope of the Study**

The main focus of the study is manufacturing and characterizing composite silica-borate nanoparticles (Si/Na-Borate) as potential lubrication additives for achieving enhanced Extreme Pressure (EP) and Antiwear (AW) properties. For this purpose, Stöber method<sup>24</sup> will be modified with the addition of Na-borate solutions instead of water. With using of silica and sodium borate in additive structure, composite nanoparticle will be attached to metal surface easily. After that, they will attach to metal surface and form ferric-borate tribofilm result in friction and wear reduction. Additionally, nanoparticles will produce with different size and morphology in order to prevent moving surfaces from contacting each other by locating into the asperities of metal.

It is expected that after the addition of this nanoparticles into lubricant material, boron oxide layer will form with attachment of boron on metal surface at first. Following that, a ferric borate layer (tribofilm) will be created by adsorption of boron into metal surface under high temperature and pressure. This tribofilm will prevent friction, wear, welding and corrosion.

Morphological (SEM, DLS) and also chemical (FTIR, XRD, ICP-MS) characterization of synthesized materials will be performed. After completing preliminary studies; parametrical studies will carry out with the final method. After optimization of the nanoparticles, dispersion and stability performance will study in different base oils with using distinctive surfactants. Finally, tribological performance of nanoparticles will measure using four ball test method in comparison with a blank base oil and a commercial lubricant.



## CHAPTER 2

### BACKGROUND AND LITERATURE REVIEW

This chapter describes chemistry and functions of lubricant additives, as well as their role in the development of advanced lubrication systems. It is conducted to give information which was readily available in literature, with the aim to show the contribution lubricant additives make towards industry, consumer and impact on the environment. This section provides an information on recent additive developments and contains recent data from the literature.

#### 2.1. Background Information

Tribology basically covers friction, wear and lubrication. When the tribology is examined etymologically, it is seen that it derives from the word "tribos" which means "rubbing". Tribology includes mechanical, chemical and material technologies. The main subject of the tribology is to reduce the friction and wear so that energy losses are reduced and life of material is extended.

Tribological systems (tribo-system) are important for machines operating under difficult conditions. A tribological system consists of four different parts. These are; two different surfaces in contact, the interface formed by these two parts and the external environment. The variables in the tribo-system are (*Figure 1*); type of motion, speed, forces acting on the system, temperature and stress.

##### 2.1.1. Friction

**Friction** (*Figure 2*) is a force against movement formed between two objects in contact. There are many types of friction; static, kinetic, slip, rolling, stick-slip and fluid friction.

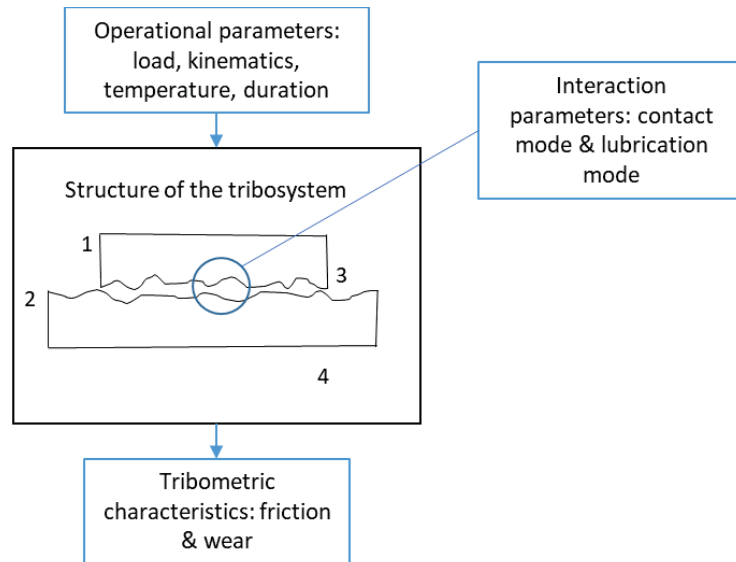


Figure 1 Structure of the tribo-system: 1, 2. Moving surfaces; 3. Intersection and lubricant; 4. Environment.<sup>11</sup>

**Static friction** (Figure 3) occurs between two objects when there is not any relative movement. **Kinetic friction** (Figure 3) is the force acting in the opposite direction to the moving object.

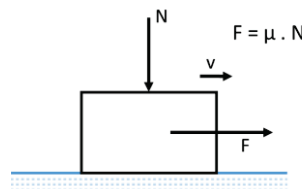


Figure 2 Coefficient of friction.<sup>11</sup>

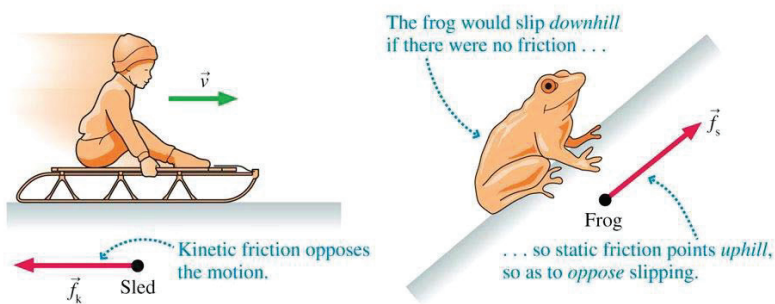


Figure 3 Kinetic Friction vs. Static Friction (Source: Pearson Education, 2017).<sup>12</sup>

**Sliding friction** (Figure 4) occurs as a result of an object slipping on the surface. **Rolling friction** is the force applied to a rolling object on a surface (Figure 4).

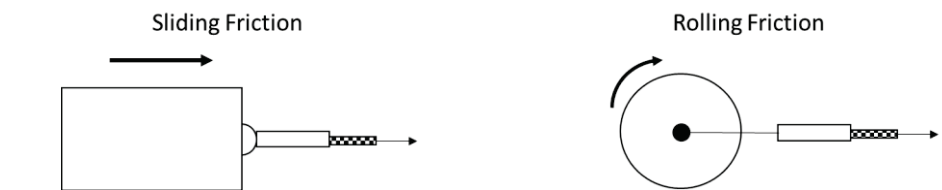


Figure 4 Sliding and rolling.<sup>11</sup>

**Stick-slip** (Figure 5) is a certain type of friction and is created by the slow contact of the floating object with another vibrating object.

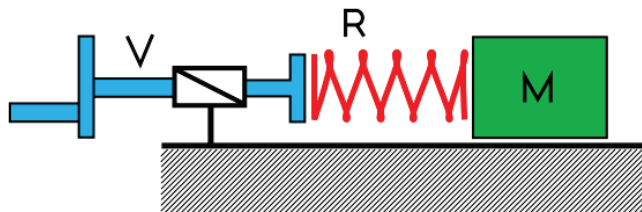


Figure 5 Engineering description of stick-slip(Source: Wikipedia, 2011).<sup>13</sup>

**Fluid friction** is generated via the movement of a solid object in liquid or gas.

Overall friction resistance in a system is mostly affected from following factors:

- Presence of particles (impurities) coming from outside the system,
- Relative stiffness of contacting materials
- Applied load
- External conditions such as temperature and presence of lubricant
- Surface topography and morphology
- Microstructure of materials
- Contact area
- Direction of movement and velocity

## 2.1.2. Wear

Wear is one of the most important cause for failure of machine elements. While friction is leading to energy loss, wear causes material loss that cannot be recovered again. It is not possible to establish a direct relationship between wear and friction. Friction resistance between different materials may be similar, but wear can be increased up to 100 times or more. Generally, wear is a more complex problem than friction. There are many different types of wear between surfaces appeared at same time. Hence, it cannot be possible to define a generalized wear law covering all wear types or part of them.

Wear can be caused by abrasion, adhesion, erosion, tribochemical reactions, surface fatigue, wear and cavitation processes (*Figure 6*).<sup>14</sup>

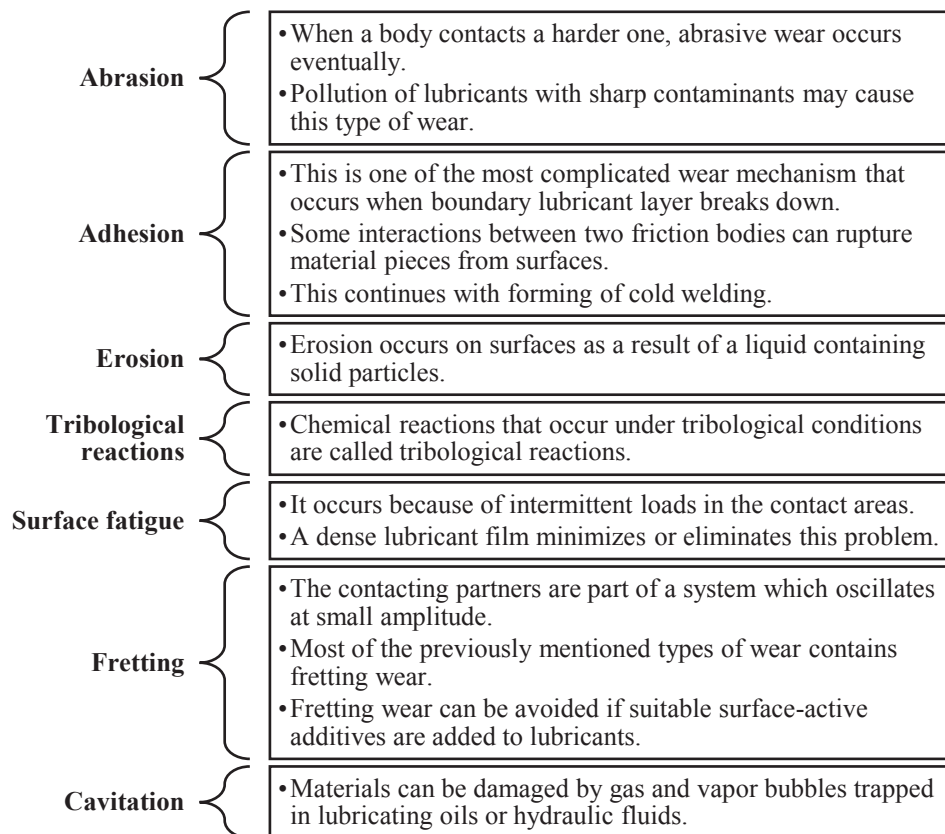


Figure 6 Types of wear.<sup>14</sup>

### 2.1.3. Fundamentals of Lubrication and Lubricants

Although the use of lubricants is as old as mankind, scientific interest on lubricants and lubrication technology is relatively new. Fundamental interest in tribology focuses to lubricant formulation, industrial operations, aerospace and transportation equipment, material shaping and machining, computers and electronic devices, power generation, and almost all phases of life where motion is encountered.

Lubricants play a crucial role in safe operation of machine elements. Main tasks of lubricants are:

- separate moving parts,
- prevent parts from heating up,
- keep the surfaces clean, and
- ensuring that the functional additives are transported to the surface.

The main objective of lubricants is to prevent surface heating, wear and friction. It is necessary to move the temperature to acceptable limits even if the parts are not completely prevented from warming up. Lubrication is also used to reduce oxidation and prevent rust <sup>15</sup>.

There are many applications that need lubricants such as transportation, industrial operations and metal working fluids. Different types of lubricants are used in these fields.

- Transportation lubricants: engine oils, power transmission fluids, brake fluids, engine coolants, and greases
- Industrial lubricants: turbine oils, compressor oils and hydraulic fluids
- Metal working fluids: metal cutting and forming fluids

Lubricants mainly consist of three different components. These are base oils, surface additives and load carrying additives. Lubrication additives can be grouped as their functions as follows (*Figure 7*).

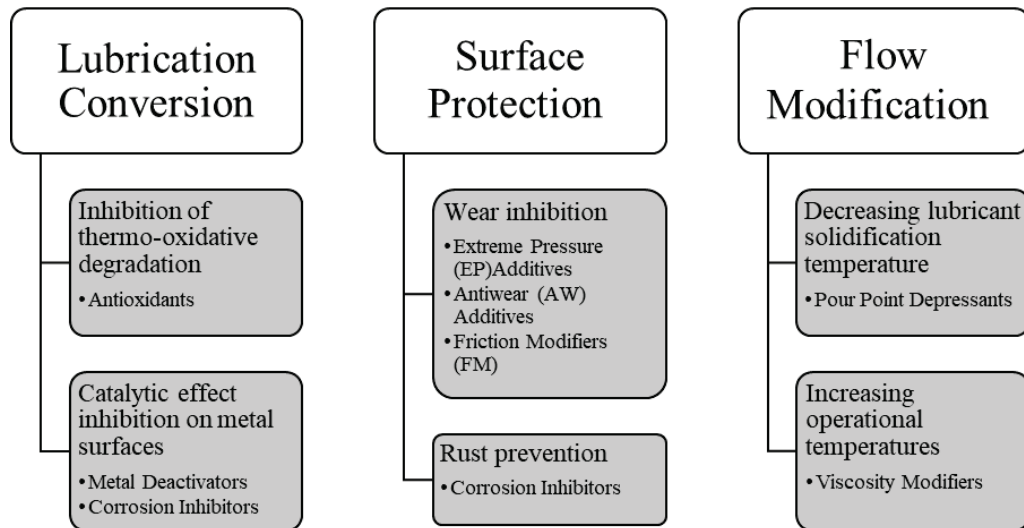


Figure 7 Functions of lubrication additives.<sup>14</sup>

#### 2.1.4. Lubrication Regimes and Stribeck Diagram

It is known that a certain resistance must be overcome to slide two surfaces under load and this resistance decreases if a lubricant is applied on surfaces. In a study published by Stribeck in 1901, it was stated that a radial sliding bearing can operate in three different regimes (*Figure 8*).<sup>11</sup> These are;

- **Boundary lubrication:** Lubricant film is not totally formed on the surface. Load is carried by asperities. EP and AW additives are active in this regime.
- **Mixed lubrication:** Lubricant film is formed with an intermediate thickness. Load is carried by both asperities and lubricant.
- **Hydrodynamic lubrication:** Moving surfaces are completely separated by lubricant film. Liquid viscosity should be high enough to preserve sufficient film thickness. Load is carried by lubricant itself.
- During the phase transition between hydrodynamic and mixed lubrication, is often referred as **Elasto Hydrodynamic Lubrication**.<sup>11</sup>

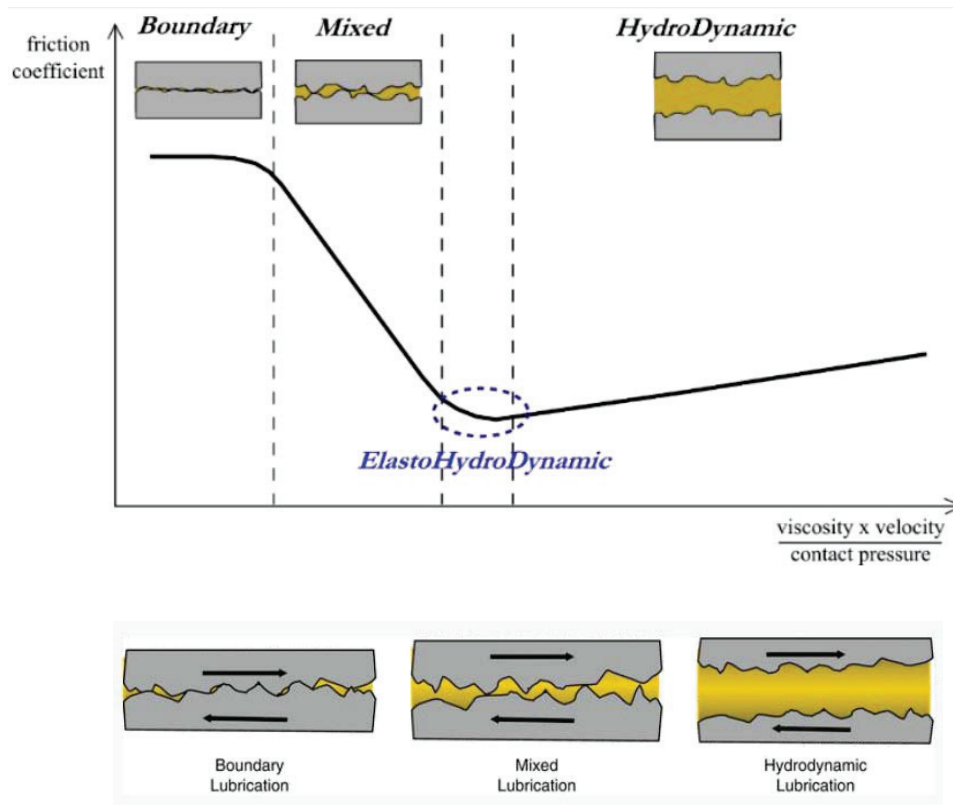


Figure 8 Stribeck diagram represents lubrication regimes (Source: Dresel et. al., 2017).<sup>11</sup>

Stribeck curve is basically between friction coefficient and bearing number. Bearing number can be described as sliding velocity, in other words relative sliding velocity of lubricant with viscosity per applied load. As seen in *Figure 8*, system does not act as a tribo-system when relative velocity is zero.

This curve is based on starting-up of a plain bearing whose shaft and bearing shells are, when stationary, separated only by a molecular lubricant layer. As the speed of revolution of the shaft increases (peripheral speed) a thicker hydrodynamic lubricant film is created what initially causes occasional mixed friction but which, nevertheless, significantly reduces coefficient of friction. As speed continues to increase a full film is formed over entire bearing surfaces; this sharply reduces coefficient of friction. As speed increases, internal friction in lubricant film adds to external friction. The curve passes a minimum coefficient of friction value and then increases, solely as a result of internal friction.<sup>11</sup>

## 2.1.5. Lubricants

Lubricants are basically a combination of base oil and additives. Additives are necessary to provide performance beyond what base oils alone are able to offer. Base oils can be considered as a carrier for the additive and a cooling medium even when the base oils also influence the performance of formulations. Base oils are five different groups defined by on saturates level, sulfur content and viscosity index (VI) properties of the oil (*Table 1*).<sup>16</sup>

Table 1 Base oil groups and characteristics<sup>16</sup>

<i>Group</i>	<i>Description</i>	<i>Sulfur Content (%)</i>	<i>Saturates Level (%)</i>	<i>Viscosity Index</i>	
<i>I</i>	Crude oil is distilled, refined physically with solvents, and may also be hydrofinished, to leave a base stock and by-products.	>0.03	<90	80-120	Lower Sulfur
<i>II</i>	Crude oil is distilled and chemically refined by hydrogenation, to leave a base stock with fewer by-products.	<0.03	>90	80-120	Higher VI
<i>III</i>	Crude oil is distilled and refined by severe cracking and hydrogenation, to produce a higher VI base stock and even fewer by-products.	<0.03	>90	>120	Purer Higher flash point
<i>IV</i>	PAO-polyalphaolefins are chemically synthesized base stocks with increased VI compared to Group III stocks.	<<0.03	>>90	>>120	
<i>V</i>	All base stocks not classified in other groups, including vegetable oil, derived base stocks, esters, diesters, glycols, etc.	<<0.03	>>90	>>120	

Traditional lubricant base stocks are derived from distillation and solvent extraction of crude oil, sourced world-wide. Alternatively the crude oil may be more highly refined using processes that include cracking and hydrotreating to produce higher quality base stocks. Some high performance formulations incorporate chemically manufactured hydrocarbons such as polyalphaolefins (PAO) and esters.



Base stock properties can differ markedly depending on the source of crude and the refining process. Lubricant additive technology provides the necessary enhancement to these base oil to achieve industry standards of performance. This increase in performance and value of formulated lubricants permits more effective use of petroleum resources.

Liquid lubricants show different physical and chemical characteristics. Physical characteristics are mainly related to the type of base oil. On the other hand, the chemical properties of lubricants are originated from the additives. Some of the outstanding characteristics are viscosity, thermal and hydrolytic stability, volatility, oxidative properties and flammability<sup>17</sup>. Properties of different base oils are placed in *Table 3* and *Table 4*.

Additionally, surface tension directly effects the lubrication. Lubricant with lower surface tension than solid surface is easily covers the surface and lead the good lubrication. Surface tension values of different base oils is listed in *Table 2*. On the other hand, surface tension of lubrication is influenced by additives. For instance, silicone containing additives in lubrication reduce surface tension drastically.<sup>17</sup>

Table 2 Surface tension of several base oils<sup>17</sup>

Liquid	Surface Tension (mN/m)
Water	72
Mineral oils	30-35
Esters	30-35
Methyl silicone	20-22
Perfluoropolyethers	19-21

### 2.1.6. Lubricant Additives

Over the last almost hundred years a number of chemical additives have been developed to enhance base oil properties, overcome their deficiencies and provide the new performance levels required by the technological evolution of machines and by the latest regulations. Many kinds of chemical additive agents are used in the manufacture of

high-quality lubricants. They are either single-purpose materials or multipurpose materials. Some commonly used additive types are described below.<sup>18</sup>

***Adhesive agents:*** Tacky, stringy materials that help form and retain uniform oil films on metal surfaces, particularly under severe conditions such as water spray.

***Antiwear agents:*** Such materials adsorb or concentrate on metal surfaces to form films that minimize the direct metal-to-metal contact. These materials should be non-staining and non-corrosive. They are typically derived from phosphorous, zinc, sulfur, boron or combinations of these elements. They are generally required when the application is operating in boundary regime.

***Defoamers:*** When added to fluids, defoamers act to alter the surface tension of a fluid to promote the rapid breakup of foam bubbles by weakening the oil films between the foam bubbles. Typically based on polysiloxanes or polyacrylates, they are effective at very low treat rates but may adversely affect air-release properties.

***Demulsifiers:*** These assist the natural ability of the oil to separate rapidly from water and also help inhibit rust.

***Detergents:*** They based on metal salts are added to oils to provide cleanliness and help reduce deposit buildup. Neutral detergents are used for cleanliness while over based detergents (high alkalinity), help neutralize any acidic buildup in the oil.

***Dispersants:*** These products help suspend solid particles in the lubricant to prevent them from binding together, thereby minimizing their precipitation as harmful deposits.

***Extreme-pressure (EP) agents:*** These materials are more active than antiwear agents and usually react with the metal surface at high temperatures to provide sufficient protection to carry even heavier loads than antiwear agents. They typically are based on sulfur or heavy metal salts.

***Friction modifiers:*** A general category of materials based on long-chain polar materials that are used to alter the frictional characteristics of a lubricant. They may be used to increase the lubricity or slipperiness where coefficient of friction may be important, or to improve fuel economy/energy conservation.

Table 3 Common properties of base oils <sup>18</sup>

LUBRICANTS	Thermal Stability (°C)	Kinematic Viscosity (cSt) at °C					Specific Gravity at 20 °C	Thermal conductivity (cal/h m °C)	Specific Heat at 38 °C (cal/g °C)	Pour Point (°C)	Flash Point (°C)	Oxidative stability (°C)	Vapor Pressure at 20 °C (torr)
		-20	0	40	100	200							
Mineral oils	135	170	75	19	5.5	0.86	115	0.39	-57	105	-	10 <sup>-6</sup> to 10 <sup>-2</sup>	
Diesters	210	193	75	13	3.3	0.9	132	0.46	-60	230	-	10 <sup>-6</sup>	
Neopentyl Polyol Esters	230	16	16	15	4.5	0.96	-	-	-62	250	-	10 <sup>-7</sup>	
Phosphate esters	240	85	38	11	4	1.09	109	0.42	-57	180	-	10 <sup>-7</sup>	
Silicate esters	250	115	47	12	4	0.89	-	-	-65	185	-	10 <sup>-7</sup>	
Disiloxanes	230	200	100	33	11	0.93	-	-	-70	200	-	-	
Silicones	280	850	250	74	25	1.03	124	0.34	-70	260	240	5x10 <sup>-8</sup>	
	260	20000		190	30	1.2	-	-	-50	290	220		
Polypheyl ethers	430	-	2500	70	63	1.18	133	0.43	-7	240	290	10 <sup>-8</sup>	
		-	-	363	13.1	2.1	-	-	+4	290			
Perfluoro Polyethers	370	-	8000	515	35	1.92	82	0.24	-30	none	320	10 <sup>-9</sup>	
		1000	440	150	41	1.87	-	0.20	-67			3x10 <sup>-12</sup>	

Table 4 Properties of different synthetic base oils <sup>18</sup>

Lubricant	Viscosity Temperature Characteristics	Volatility	Oxidation resistance	Thermal Stability	Lubrication Characteristics	Solubility in petroleum and other characteristics	Improvement additive compatibility	Typical Applications
<b>Chloro fluoro-carbons</b>	Poor	Some lower, some higher	Excellent	Poor to excellent	Good to excellent	Generally poor	Widely variable	Nonflammable, extreme oxidation-resistant lubricants for plant processes of devices handling reactive materials
<b>Dibasic-acid ethers</b>	Good to excellent	Generally lower	Fair to good	Fair to good	Fair to good	Good to excellent	Generally good	Instrument oils, low-volatility grease bases, special hydraulic fluids, gas turbine lubricants
<b>Nonpently polyol ethers</b>	Good to excellent	Lower	Good	Good	Fair to good	Good to excellent	Generally good	Instrument oils, low-volatility grease bases, special hydraulic fluids, gas turbine lubricants
<b>Polyglycol ethers</b>	Good to excellent	Generally lower	Poor to fair	Fair to good	Good	Fair to good	Generally good	Special hydraulic fluids, forming and drawing lubricants, low-temperature grease base, vacuum-pump lubricants, components of other synthetic lubricant formulations
<b>Phosphate esters</b>	Excellent	Generally lower	Good	Fair to good	Good to excellent	Good to excellent	Generally good	Fire resistant hydraulic fluids, low-volatility, high-lubricity grease base, lubrication additives in other synthetics, special low-temperature lubricants
<b>Silicones</b>	Excellent	Much lower	Good to excellent	Good to excellent	Poor to fair	Poor	Poor	High temperature bearings, condensation pump lubricant, low-volatility grease base for lightly loaded bearings, damping fluids, devices requiring minimum viscosity change with temperature
<b>Silanes</b>	Fair to good	Much lower	Fair to good	Good to excellent	Fair to good	Fair	Fair	Base stocks for high-temperature greases, hydraulic fluids, and engine lubricants; require extensive formulation
<b>Polyphenyl ethers</b>	Poor to fair, generally high pour points	Much lower	Excellent	Excellent	Fair to good	Fair	-	High-temperature fluid for reactor coolant, hydraulic applications at very high temperatures
<b>Perfluoro poly-ethers</b>	Good to excellent	Lowest	Excellent	Excellent	Good	Fair	-	Base stocks for high-temperature, vacuum and chemical resistance applications; hydraulic fluids for very high temperatures, magnetic rigid disks

***Metal passivators:*** These materials help to minimize the catalytic action of certain surfaces; for example, copper-based tubes may oxidize oil unless coated with a passive coating.

***Oxidation inhibitors:*** Some additive agents function as peroxide decomposers, chain stoppers, and/or metal deactivators. Peroxide decomposers destroy the precursor of radical sources by converting the peroxides into harmless compounds. Chain stoppers interrupt the chain reaction between oxygen and hydrocarbon radicals to prevent or slow the formation of acidic materials, propagated materials and sludge. Metal deactivators retard the oxidation-promoting catalytic effect of metals in a lubricating system. The metal surfaces or particles are covered by the agent, which acts as a barrier to prevent the catalytic effect. The most catalytically active metal is copper, the second is lead and the third is iron.

***Pour-point depressants:*** These improve the low-temperature fluidity of mineral oils and reduce wax formation at low temperatures.

***Rust inhibitors:*** Most lubricating oils contain rust inhibitors to enhance their ability to minimize rusting. They typically are based on calcium sulfonate or alkylated succinic acids.

***Seal swell agents:*** These are fluids that help modify the swelling characteristics of elastomers. They are typically required where high levels of highly paraffinic base oils are used. Esters and alkylated naphthalene can be used in this role.

***Viscosity index improvers:*** When added to oils, these high-molecular-weight polymers improve the viscosity index by coiling and uncoiling in response to temperature. They may help lower the pour point at low temperature while providing sufficient viscosity at high temperature. They can be subject to breakdown through thermal or mechanical stress.

### 2.1.7. Antiwear and Extreme Pressure (EP) Additives

Extreme pressure (EP) and antiwear additives are used to separate metal surfaces in the case of heavy loading and reduce wear mainly in boundary lubrication condition, where metal-to-metal contact is observed. EP and AW additives operate in metalworking fluids, engine oils, hydraulic fluids or lubricating greases resulting in a tribochemical reaction of additives on the metal surface.

These additives that contain polar structures create films on the metal surface by adsorption or chemisorption, which guarantees their function under boundary and/or mixed lubrication regimes. AW and EP additives can react with the metal surface in order to form tribochemical reaction layers (tribofilms, *Figure 9*) these can be iron phosphides, sulfides, sulphates, oxides and carbides. Tribofilms avert the connection between the moving surfaces. These layers can soften the roughness of the metal surface and reduce wear due to micro-welding processes. Tribofilms also avoid the actual welding of sliding parts under extreme pressure conditions.

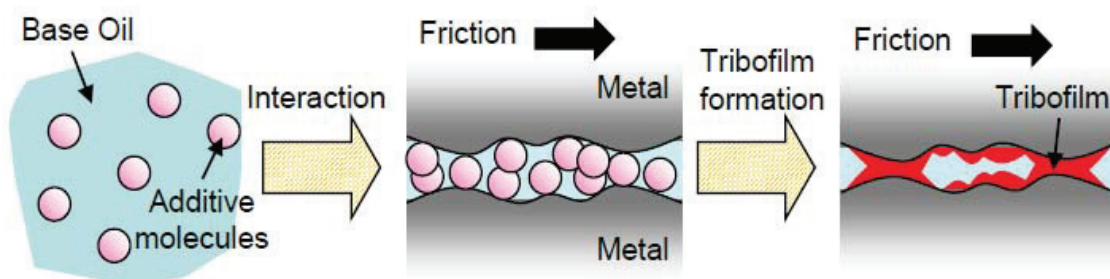


Figure 9 Tribofilm formation on metal surfaces (Source: Shah et. al., 2009).<sup>19</sup>

A clear distinction between AW and EP additives are not always so clear due to the various types of chemistries used in differing applications. However, AW additives generally deposit chemical layers on the metal surface during normal operating conditions. EP additives on the other hand become active when the system comes under serve stress, to prevent the welding of moving parts. *Table 5* shows brief comparison of these additives.

Some popular AW additives are:

- Zinc dithiophosphate (ZDP)
- Zinc dialkyl dithio phosphate (ZDDP), probably the most widely used in formulated engine oils, also acts as a corrosion inhibitor and antioxidant
- Tricresyl phosphate (TCP), used for high-temperature operation, often used as an AW and EP additive in turbine engine lubricants, and also in some crankcase oils and hydraulic fluids
- Halocarbons (chlorinated paraffins), for extreme pressure operations
- Glycerol mono oleate
- Stearic acid, adhering to surfaces via reversible adsorption process under 150 °C, which limits its use to mild contact conditions.

Table 5 Differences of EP and AW additives<sup>21</sup>

<b>AW Additives</b>	Polar additives that attach to metal surfaces
	React chemically with the metal surfaces during metal-to-metal contact
	Activated by heat of contact/form a minimizing wear
	Protects surfaces from wear during boundary lubrication
	Protect base oil from oxidation and metal from damage by corrosive acids
	Typically P compounds (ZDDP)
	<b>EP Additives</b>
More chemically aggressive than AW additives.	
Adsorb to metal surfaces to form a sacrificial film that prevents the welding	
Activated at high loads and by the high contact temperatures that are created	
Mostly S and P compounds; rarely chlorine-based due to corrosion concerns	

Many AW additives function as EP additives, for example organophosphates or sulfur compounds. Under extreme pressure conditions, the performance of AW additives becomes insufficient and designated EP additives are required.<sup>20</sup>

EP additives are usually used in applications such as gearboxes, while AW additives are used with lighter load applications such as hydraulic and automotive engines.

EP additives typically contain organic sulfur, phosphorus or chlorine compounds which chemically react with the metal surface under high pressure conditions. Under such conditions, small irregularities on the sliding surfaces cause localized flashes of high temperature (300-1000 °C), without significant increase of the average surface temperature. The chemical reaction between the additives and the surface is confined to this area.

The early EP additives were based on lead salts of fatty acids ("lead soaps"), "active sulfur" compounds (e.g. thiols and elementary sulfur), and chlorinated compounds. During the 1950s the use of lead soaps was eliminated and replaced by zinc and phosphorus compounds such as zinc dialkyl dithio phosphate (ZDDP).

Some of the EP additives are:<sup>22</sup>

- Dark inactive sulfurized fat
- Dark active sulfurized fat
- Dark active sulfur hydrocarbon
- Short and medium chain chlorinated alkanes
- Esters of chlorendic acid
- Polymer esters
- Polysulfides
- Molybdenum compounds

## **2.2. Literature Review**

This part presents an overview on the use of various classes of nanomaterials in lubricant formulations also limitations of conventional additives. Current advances in using different nanomaterials in lubricants such as engine oils, industrial lubricants and greases are stated.



## 2.2.1 Conventional AW and EP Additives

Conventional additives often contain compounds of metals, sulfur, and phosphorus; for example, ZDDPs. Despite their good AW performance, friction is actually increased, which is a problem if machine efficiency is to be improved. The presence of zinc and large amounts of sulfur and phosphorus in engine oils leads to degradation of the exhaust catalyst systems in automobiles. This results in the emission of toxic exhaust gases and hazardous particles. Future environmental legislation is expected to significantly reduce limits on pollutants. The efficiency of catalyst systems must consequently be enhanced. This is hardly possible without developing more efficient lubrication solutions.<sup>23</sup>

***Sulfur Additives:*** EP performance of a sulfur additive is directly proportional to sulfur content. Sulfur additives can be used together with phosphoric acid esters to enhance their properties. Tribofilm formation process of sulfur carriers under extreme conditions starts with physisorption, continue with chemisorption and finalized with sulfur-metal reaction at above 600 °C (*Figure 10*).<sup>24</sup>

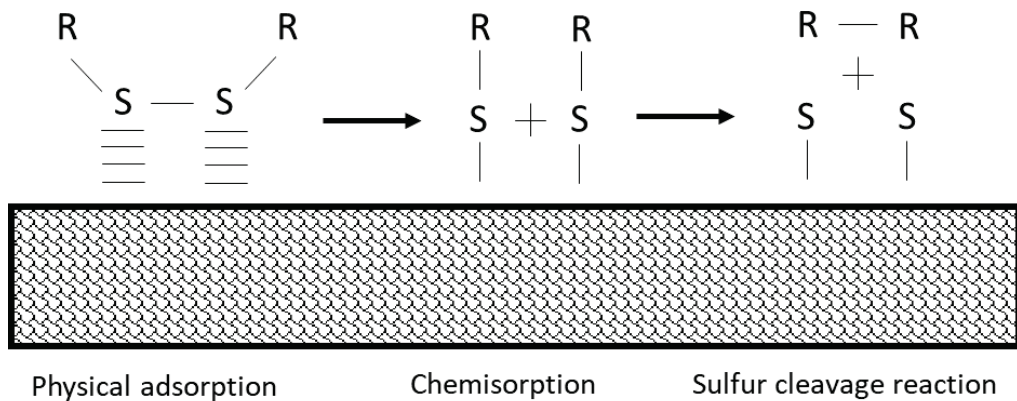


Figure 10 Tribochemical attractions of sulfur additives under extreme conditions.<sup>24</sup>

General formula of sulfur derivatives is  $R-S_x-R$ . When  $x$  equals to 2, additives are called “inactive sulfur carriers”, otherwise  $x$  is between 3 and 5 that named as “active sulfur carriers”. Inactive types react only at high temperatures, but active ones are more reactive and easily bond even at low temperatures.

Sulfur-containing additives mainly contain sulfurized olefins, sulfurized esters, sulfurized oils, dibenzyl disulfide (DBDS), butyl phenol disulfide, diphenyl disulfide and tetra methyl dibenzyl disulfide.<sup>24</sup>

**Phosphorus Additives:** Phosphorous additives prevent metal-metal connection from medium to high pressure range when used in boundary lubrication. Unlike sulfur additives, phosphorus additives generally have better corrosion protection. Due to completely different film formation mechanisms, phosphorus additives cannot be used as substitution of sulfur additives or vice versa. Consistently, phosphorus additives are highly effective in low shear rates and with surfaces have high surface roughness. Under moderate stress conditions, organic phosphorus derivatives used perfectly as antiwear additives.

The main phosphorus additives are phosphate esters, phosphides, dialkyl phosphonates and acid phosphates.<sup>24</sup>

**Sulfur-Phosphorus (S/P) Additives:** These additives can be used to avoid metal-metal connections, at medium to high pressure, in boundary lubrication conditions. Metallic S/P additives are the most important AW/EP additives used for engine lubrication.<sup>24</sup>

Zinc dialkyldithiophosphates (ZDDP) is the most important and well-known additive group of sulfur-phosphorus compounds (*Figure 11*).

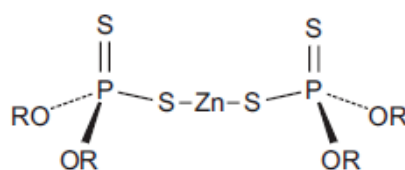





Figure 11 Structure of ZDDP (Source: Dresel et. al., 2017).<sup>24</sup>

Thermal stability and chemical affinity (AW/EP performance) of ZDDPs are affected from formation of alkyl groups. Thus, thermal stability rises with chain length of alkyl groups and their structures in secondary, primary and aromatic sequences. Effect of alkyl structures on the properties of ZDDP is shown in *Figure 12*.<sup>24</sup>

ZDDPs often work as AW additive but their EP properties are not sufficient. As an AW additive, ZDDP works under boundary (and also mixed) lubrication condition and separates metal surfaces. Thickness and composition of tribofilm are straightly depends on temperature and friction conditions of the surface. As temperature increases, ZDDP decomposes into dialkyldithiophosphoryl disulfide and adsorbs into metal surface. Similarly, when load is sufficient to eliminate lubricant film on the surface, ZDDP reacts with metal to avoid welding and decrease wear (*Figure 13*).<sup>26</sup>

Alkylgroup R	Reactivity (antiwear properties)	Thermal stability	Hydrolytic stability	Antioxidant properties
R = C <sub>3</sub> ↓ R = C <sub>8</sub>	 + -	 - +	 - +	No systematic influence
Structure of R				
Primary alkyl	+/-	+	+/-	+/-
Secondary alkyl	++	-	+	+
Aryl	--	++	--	-

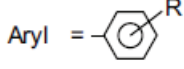
Primary alkyl group =  $-\text{CH}_2-\text{R}$   
 Secondary alkyl group =  $-\underset{\text{R}'}{\text{C}}\text{H}-\text{R}$   
 Aryl = 

Figure 12 The effect of the alkyl structure on the properties of ZDDP (Source: Dresel et. al., 2017).<sup>24</sup>

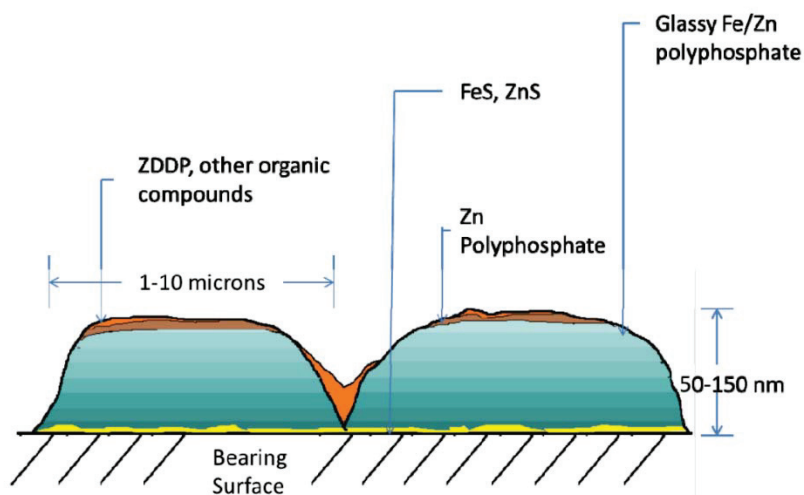


Figure 13 Structure of ZDDP tribofilm on metal surface (Source: Johnson et. al., 2013).<sup>25</sup>

**Sulfur–Nitrogen (S/N) Additives:** In boundary lubrication and at extreme pressures, S/N additives provide protection against metal-metal interactions. Dithiocarbamates are commonly used S/N additives. Additionally, heterocyclic compounds such as 2,5-dimercapto-1,3,4-thiadiazole (DMTD), 2-mercapto-1,3-benzothiazole (MBT) and derivatives can be used as antioxidants, corrosion inhibitors and metal passivation agents.<sup>24</sup>

**Phosphorus-Nitrogen (P/N) Additives:** P/N additives are used in medium to high pressure range to avoid metal-metal connections. Ashless P/N compounds are commonly used as bifunctional antifoam / anticorrosive additives, and the most commonly ones are amine dithiophosphates, amine thiophosphates, amine phosphates and phosphor amides.<sup>24</sup>

**Complex Additives:** They are composed of S/P, S/N, P/N compounds and many others. There are many examples of complex additives in the market; such as amine salts of dithiophosphates and thiophosphates, borate derivatives of dithiophosphates, dithiocarbamates and dimercaptothiadiazole, urethane derivatives of dithiophosphates, and derivatives of dialkyl phosphites, sulfur and acylated amines.<sup>24</sup>

**Halogen Additives:** Chlorine has been used as an AW additive for many years. Especially, chlorine combines with sulfur compounds in metal working fluids. Additionally, iodine is used for wear reduction in aluminum processing oils. It is well known that fluorinated, perfluorinated compounds reduce wear. Effect of chlorine additives directly related to reactivity, temperature and concentration of chlorine atom. Chlorine additives can cause corrosion on metal surfaces due to formation of hydrogen chloride in existence of moisture. Due to environmental impact and toxicity, chlorine additives are restrictedly used even if they are highly effective as additives.

### **2.2.2. Novel AW and EP Additives-Nanoparticles in Lubricants**

Instead of traditional materials, new nanomaterials and nanoparticles have been recently under investigation as lubricants or lubricant additives because of their unusual properties. Their characteristic size will allow them to enter the contact region. Also they are small enough to pass undisturbed through filters used in oil systems. In comparison

with organic additives, nanoparticles are considered thermal stable at elevated temperatures that makes them favorable as lubricant additives. Some other of the advantages of using nano-additives are maintaining variety of particle chemistries, and reaction rate with the surface without an induction period, which is an important factor for conventional lubricant additives.<sup>26,27</sup>

Based on the *Table 6*, reported nanoparticles that used as lubricant additives can be divided into seven types based on their chemistry: carbon and its derivatives, metals, metal oxide, sulfides, rare earth compounds, nanocomposites and others. Detailed information about each category is listed in *Table 7*.

For carbon and its derivatives, molecular structures (sheet, tube, onion) played a dominant role in determining their tribological behavior. For metals and metal oxides, the majority elements were located in the transition metal group. For sulfides, the representative one was MoS<sub>2</sub>, others included WS<sub>2</sub>, CuS, and NiMoO<sub>2</sub>S<sub>2</sub>. For rare earth elements, Y, La, and Ce were considered as favorable elements for lubricant additives. For nanocomposites, they were the combinations of the aforementioned several categories. Others included CaCO<sub>3</sub>, ZnAl<sub>2</sub>O<sub>4</sub>, Zeolite, ZrP, SiO<sub>2</sub>, PTFE, Hydroxide, BN, serpentine, and among others.

Several factors affect tribological performance of nanoparticles on oil lubrication. Chemical composition of nanoparticles played an important role on antiwear performance, while had a subtle effect on frictional performance. Wear resistance was closely related with the properties of the tribofilm in boundary lubrication regime. Metals were favorable of tribofilms. The size of nanoparticles showed visible effects on both friction and wear. Size optimization was governed by the specific working conditions and lubrication regimes. Morphology of nanoparticles played a critical role on friction reduction, while had a subtle effect on antiwear performance. Frictional performance was more likely to be related to the physical interaction between the nanoparticles and environment. Antiwear performance was mostly related to the chemical interaction between nanoparticles and environment.<sup>28</sup>

Table 6 Summary of nano-sized lubricant additives<sup>28</sup>

Ag doped MoS <sub>2</sub> nanoparticles	MoS <sub>2</sub> and SiO <sub>2</sub>
Ag nanoparticle	Diamond and graphene
Al <sub>2</sub> O <sub>3</sub>	Nano-Cu / graphene oxide composites
Al <sub>2</sub> O <sub>3</sub> and Cu	Nano-PTFE
Al <sub>2</sub> O <sub>3</sub> / SiO <sub>2</sub> composite	Ni
Al <sub>2</sub> O <sub>3</sub> / TiO <sub>2</sub> nanocomposite	NiMoO <sub>2</sub> S <sub>2</sub>
Bismuth nanoparticles	Ni based nanolubricants
BN	OA/La-TiO <sub>2</sub>
Calcium carbonate nanoparticles	Pd
CeO <sub>2</sub>	Pd and Au nanoparticles
Cu	PTFE
Cu nanoparticles in serpentine powders	Rhenium doped MoS <sub>2</sub>
Cu / SiO <sub>2</sub> nanocomposites	SA/CeBO <sub>3</sub>
CuO	Serpentine ultrafine powders
CuO, TiO <sub>2</sub> and nanodiamond	Serpentine , La(OH) <sub>3</sub> and their composites
CuS	Single wall carbon nanohorns (SWCNH) and TiO <sub>2</sub>
Diamond and SiO <sub>2</sub>	SiO <sub>2</sub>
Diamond nanoparticles	Sn and Fe nanoparticles
Fe, Cu, Co NPs	TBP-LaF <sub>3</sub>
Fe <sub>3</sub> O <sub>4</sub> magnetic NPs	TiO <sub>2</sub>
Fullerene-like MoS <sub>2</sub> nanoparticles	Ti, CuO, Al <sub>2</sub> O <sub>3</sub> , MWNTs
Graphene and MoS <sub>2</sub> compresion	Titanium nanoparticles
h-BN	Zeolite
Hydroxides NPs (Mg/Al/Ce/LDHs)	ZnAl <sub>2</sub> O <sub>4</sub>
IF-MoS <sub>2</sub> nanoparticles	ZnO
IF-WX <sub>2</sub>	ZnO and CuO
La doped Mg/Al LDH	ZrO <sub>2</sub>

Table 7 Types of nanoparticles as lubricant additives<sup>28</sup>

Types	Nanoparticles
Carbon and its derivatives	Graphene, diamond, SWCNT, MWCNT
Metals	Sn, Fe, Bi, Cu, Ag, Ti, Ni, Co, Pd, Au
Metal oxide	ZrO <sub>2</sub> , TiO <sub>2</sub> , Fe <sub>3</sub> O <sub>4</sub> , Al <sub>2</sub> O <sub>3</sub> , ZnO, CuO
Sulfides	WS <sub>2</sub> , CuS, MoS <sub>2</sub> , NiMoO <sub>2</sub> S <sub>2</sub>
Rare earth compounds	LaF <sub>3</sub> , CeO <sub>2</sub> , La(OH) <sub>3</sub> , Y <sub>2</sub> O <sub>3</sub> , CeBO <sub>3</sub>
Nanocomposites	Cu/SiO <sub>2</sub> , Cu/Graphene oxide, Al <sub>2</sub> O <sub>3</sub> /SiO <sub>2</sub> , serpentine/La(OH) <sub>3</sub> , Al <sub>2</sub> O <sub>3</sub> /TiO <sub>2</sub>
Others	CaCO <sub>3</sub> , ZnAl <sub>2</sub> O <sub>4</sub> , Zeolite, ZrP, SiO <sub>2</sub> , PTFE, Hydroxide, BN

Based on literature nanoparticles were collected in *Table 6*, number of studies about one particularly type was plotted in a pie chart as shown in *Figure 14*. As seen that the majority of nanoparticles that used as lubricant additives consisted of metal oxides, metals and sulfides.

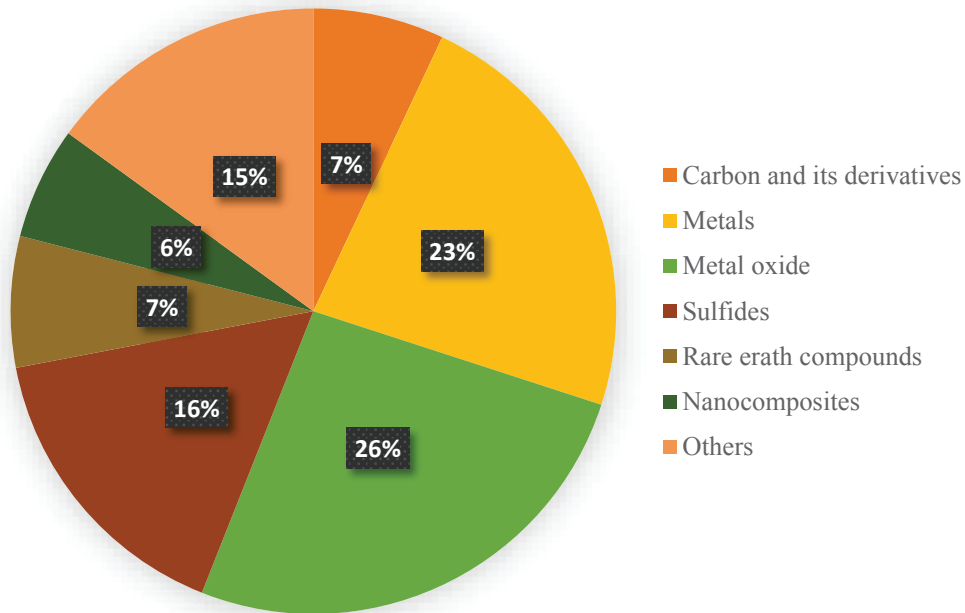


Figure 14 Statistics of nanoparticles worked as lubricant additives.<sup>28</sup>

There are many experimental studies that have reported tribofilm formation mechanism for superior lubrication. The formation of this tribofilm can be characterized using analysis techniques like scanning electron microscopy/energy dispersive spectrometer (SEM/EDS), Raman spectroscopy, and X-ray photoelectron spectroscopy (XPS), as given in *Table 8*.

A number of lubrication mechanisms have been reported in the literature in terms of primary direct effect (ball bearing/tribo-film) and secondary surface enhancement (mending/polishing). Although a number of surface analysis techniques have been used in a variety of articles, the explanation of lubrication mechanisms of nanoparticles-based lubrication remains unclear and even mystifying in few cases. The complexity of lubrication mechanism increases for fully formulated lubricants as no such study has discussed the chemical interaction between existing additives and nanoparticles.

### 2.2.3. Boron Compounds as AW and EP Additives

Boron compounds are extensively used as friction modifiers (FM), antiwear and extreme pressure (EP) additives in many types of environmentally friendly lubricants.<sup>23</sup>

Boron is a multifunctional compound that is used as;

- ❖ solid lubricant such as boric acid and hexagonal boron nitride,
- ❖ liquid lubricant such as ionic liquids,
- ❖ lubricant additive such as borate derivatives of various organic and inorganic compounds, and
- ❖ coating such as cubic boron nitride and different metal borides.

Unlike other tribological compounds, the versatile chemistry of B makes it effective additive for both solid and liquid lubricants. Boron derivatives are prone to interact with different types of materials at different temperatures and pressures. Additionally, starting materials used for synthesis of new boron species are naturally occurring and low-cost chemicals. These properties might therefore facilitate the commercialization of boron based lubricants for various tribological applications from both economic and environmental points of view.

The excellent tribological properties of the boron compounds can be listed as follows.<sup>23</sup>

- ✓ Boron compounds can be transformed into reactive species containing boron at high temperature and pressure
- ✓ It has been observed that the elemental boron interacts with positively charged metal surfaces by being partially negative loaded under pressure.
- ✓ As a result of the decomposition of the oils containing boron compound, the metal surfaces are formed by ferric boride ( $\text{FeB}$  and  $\text{Fe}_2\text{B}$ ) and high adhesion resistant abrasion resistant film layers are formed.
- ✓ Boron compounds create graphite-like structures on hard ferric boride and ferric nitride films to reduce creep coefficient.



Table 8 Summary of reported effects of nanoparticles on tribological properties<sup>29</sup>

<i>Particle</i>	<i>Lubricant</i>	<i>Nanoparticle Role</i>	<i>Mechanism</i>	<i>Surface Analysis Technique</i>
<i>Cu</i>	PAO6	AW, EP	Tribosinterization	SEM, EDS
<i>Ni</i>	-	FM, AW, EP	Tribosinterization	SEM, EDS
<i>ZnO, ZrO2, CuO</i>	-	AW, EP	Deposition	SEM, EDS
<i>Graphite</i>	Supergear EP220	FM, AW	Polishing	SEM, AFM
<i>Fulleren, Carbon nanoballs</i>	SAE-20W50	AW	Mending	SEM
<i>Al/Sn</i>	SE15W/40	AW, EP	Mending	SEM, EDS
<i>Pb</i>	TBA, Liquid paraffin	FM, AW	Ball bearing Tribofilm	SEM, EDS
<i>Fe, Cu, Co</i>	SAE10	FM, AW	Tribofilm	SEM, EDS
<i>Al</i>	Liquid paraffin	FM, AW	Tribofilm	SEM, EDS
<i>CuO</i>	SAE30	FM, AW	Ball bearing Mending	SEM, EDS
<i>CuO, MoS2</i>	Mineral oil Liquid paraffin Palm TMP ester	FM, AW FM, AW AW, EP	Deposition, Polishing Ball bearing Mending, Tribofilm	SEM, EDS - SEM, EDS, Raman Spectroscopy
<i>BN, MoS2</i>	PAO10	FM, AW	Tribofilm	Raman Spectroscopy
<i>MoS2</i>	SAE 20W-40 PAO Liquid paraffin	FM, AW, EP FM, AW, EP FM, AW, EP	Mending Tribofilm Tribofilm	SEM, EDS SEM, EDS SEM, EDS
<i>MoS2, TiO2, MoS2/TiO2</i>	Liquid paraffin	FM, AW	Mending, Tribofilm	XPS
<i>ZnO</i>	60SN bade oil	FM, AW	Mending	SEM
<i>h-BN</i>	SAE 15W40	FM, AW	Ball bearing, Polishing	SEM
<i>Magnesium borate</i>	500SN base oil	FM, AW, EP	Deposition, Tribofilm	SEM, XPS
<i>Al2O3</i>	SAE 15W40	FM, AW	Ploughing effect	SEM
<i>WS2</i>	Jatropha TMP ester	AW, EP	Tribosinterization	SEM
<i>ZnO, CuO</i>	Mineral oil PAO Sunflower oil Soybean oil	FM, AW FM, AW FM, AW FM, AW	Deposition, Tribofilm Deposition, Tribofilm Tribofilm Tribofilm	SEM, EDS SEM, EDS SEM, EDS SEM, EDS
<i>Tio2</i>	10W-30	FM, AW	Ball bearing, Deposition	-
<i>ZnAl2O4</i>	Lubricating oil	FM, AW	Self-repairing effect, Mending	SEM, EDS

Boron provides excellent lubrication with two main mode of action at the interface.<sup>23</sup>

1. Boron, oxygen and nitrogen by interacting with the surface of boron oxide and boron nitride, such as low friction coefficient and creates slippery layers.
2. It creates super hard materials such as metal borides which interact with boron metals and minimize surface wear.

A wide range of boron compounds as potential lubricant additives can be designed and synthesized, thanks to the unique chemical nature and reactivity of boron. There are many different studies related boron compounds in the field of tribology. As seen in *Figure 15*, there has been an increasing interest in studies involving boron-containing additive in recent years. Specifically, borate derivatives, boric acid and h-BN have been extensively studied. But, there is not any study related the usage of borates and silica together in literature.

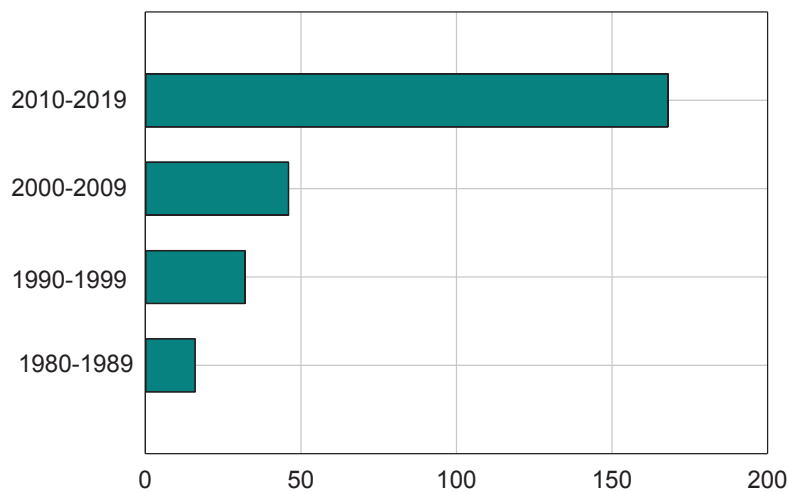


Figure 15 Number of articles in Web of Science (Keywords: boron/ borate/ boric acid /friction/ lubricant/ EP/ AW)

Borate derivatives are highly slippery due to their crystal structure. Borates consist of crystal layers in which atoms are tightly bonded to each other. Thanks to these structures, the friction coefficients are low. The layers are relative to one another and are linked by molecular bond (van der Waals). Under stress, these layers slip easily on each other. This reduces friction and increases wear resistance. Borates can be used with

friction reduction aspects in lubricants instead of phosphate derivatives (ZDDP). It is difficult to disperse borate nanoparticles in base oils. To solve this problem, dispersants can be added to the formulations or surfaces of the nanoparticles can be modified.

Mostly studied inorganic borate derivatives as AW and EP additives are; calcium borate,<sup>2-4</sup> lanthanum borate,<sup>5</sup> magnesium borate,<sup>6, 30</sup> strontium borate,<sup>31</sup> zinc borate,<sup>8, 32, 33</sup> cerium borate<sup>10</sup> and titanium borate.<sup>34</sup> There is some detailed information about these borate compounds in *Table 9*.

Table 9 Literature review of borate nanoparticles

Nanoparticle	Size (nm)	Technique	Wear resistance	Friction coefficient	Tribofilm composition
Mg-Borate	10	supercritical fluid drying	improved	decreased	FeB
Ca-Borate	70	supercritical fluid drying	improved	decreased	B <sub>2</sub> O <sub>3</sub> , CaO and iron oxides
Ca-Borate	50-200	sol-gel precipitation	improved	decreased	B <sub>2</sub> O <sub>3</sub> and FeB
Ca-Borate	50-100	sol-gel precipitation	improved	decreased	B <sub>2</sub> O <sub>3</sub> , FeB, Fe <sub>2</sub> O <sub>3</sub> and CaO
Ce-Borate	50	sol-gel precipitation	-	slightly decreased	-
Ti-Borate	10-70	supercritical fluid drying	improved	decreased	B <sub>2</sub> O <sub>3</sub>
Zn-Borate	20-50	supercritical fluid drying	improved	decreased	B <sub>2</sub> O <sub>3</sub> , FeB and Fe <sub>2</sub> B
La-Borate	20-40	replacing solvent dry	improved	-	B <sub>2</sub> O <sub>3</sub> and FeB
Sr-Borate	50-250	supercritical fluid drying	improved	slightly decreased	FeB and FeB <sub>2</sub>

Sodium borate (Na-Borate) was used as a boron source for all studies in *Table 9*. Common method to synthesize nanoparticles is supercritical fluid drying technique using ethanol. Size of nanoparticles vary between 10-250 nm. Generally, wear resistance was improved and friction coefficient was decreased. Composition of tribofilm was characterized commonly by using XPS.

With the ascending interest of the usage of nanoparticles as lubricant additives has forced researchers to work with boric acid. As seen in the literature, micronized boric acid can decrease the friction coefficient of ceramic and metal surfaces drastically. On the other hand, nano boric acid is preferred as a lubrication additive for automotive industry. However, nano-boric acid is prone to agglomerate in the existence of water. This problem causes particle size increase and flocculation of the particles in the base oil. Although,

different surfactants can be used to prevent this problem, agglomeration problem cannot be eliminated but only minimized. Therefore, new boron based nanoparticle technology is needed to create stable dispersions even in the presence of water and other potential pollutants.<sup>28</sup>

Boric acid interacts with metallic surfaces in the existence of water vapor. As a result of this interaction, a boron oxide layer is formed on the metal surface and this layer is a corrosion resistant barrier. When this layer is formed, boron oxide is converted into boric acid simultaneously. Boric acid molecules are in the form of crystalline layers. While these layers are connected to each other by weak bonds, they are covalently bound in themselves. Because of mechanical forces, boric acid layers, which are connected with van der Waals forces, slide over each other and reduce friction (*Figure 16*). Boric acid can form anti-friction and -wear layers even at temperatures as high as 1000 °C (the temperature at which the lubricants are completely decomposed).<sup>23</sup> In cases where boric acid was used, friction decreased by 80% and abrasion decreased by up to 90%.<sup>27</sup> Boric acid is highly compatible with other lubricant additives. They can be used as an environmental alternative instead of conventional lubricant additives containing sulfur.

Hexagonal boron nitride (h-BN) is a well-known lamellar solid lubricant like. Its structure is very similar to that of graphite and due to its white color, it is sometimes referred to as “white graphite”. In its layered structure, boron and nitrogen are covalently bonded to one another to form a two-dimensional atomic sheet, while bonding between the layers is primarily van der Waals type and weak (*Figure 17*). It is chemically stable and thermally resistant to oxidative degradation up to ~1000°C. It is used as a solid lubricant at elevated temperatures. h-BN has self-lubricity and its performance is better than other solid lubricants (molybdenum dioxide, zinc oxide, graphite, etc.).

There is limited applications related using silica nanoparticles in tribological applications. In Badia-Laino et al.’s study,<sup>36</sup> silica nanoparticles (SiO<sub>2</sub> NPs) synthesized by the sol–gel approach and modified by grafting hydrophobic chains (*Figure 18*) to prevent their aggregation and improve their dispersibility in lubricant base oils. Long alkane chain-hybrid SiO<sub>2</sub> NPs have been demonstrated to reduce the friction coefficient and wear. This reduction implies a strong reduction in spend of energy as a consequence of the friction processes, thus also reducing the cost of lubrication.

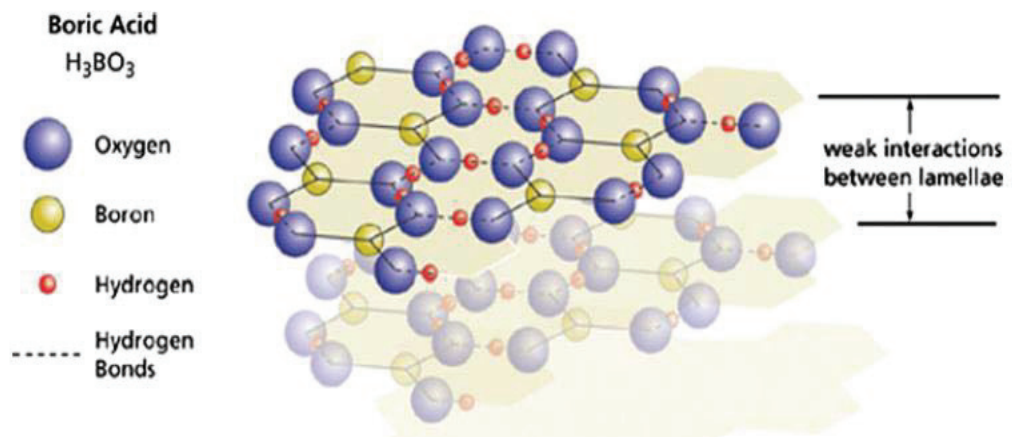


Figure 16 Structure of boric acid (Source: Shah et. al., 2013).<sup>23</sup>

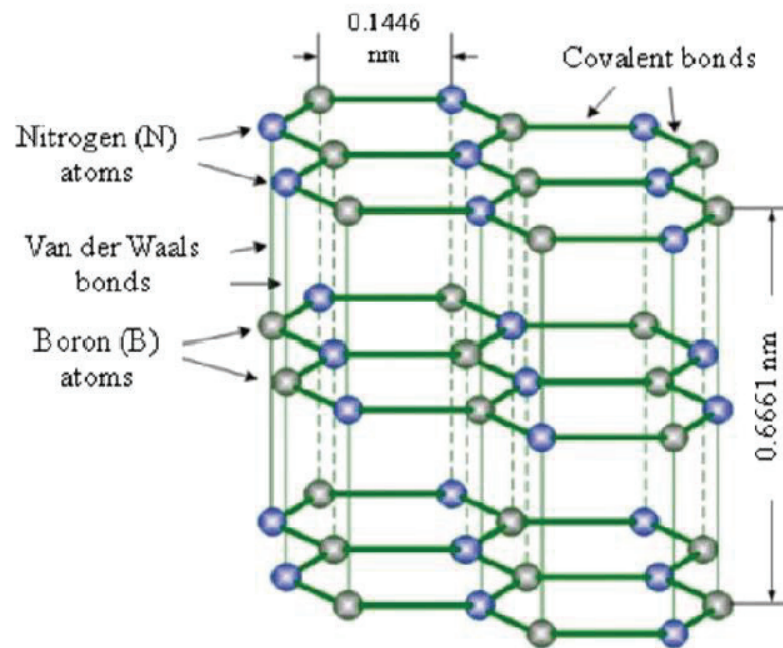


Figure 17 Structure of h-BN (Source: Hu et. al., 1998).<sup>35</sup>

In another study performed by Song et.al,<sup>37</sup> silica nanoparticles with different sizes and amino group organic chains were synthesized and dispersed in polyalphaolefin (PAO). It was found that the HSNs could form a stable homogeneous solution with PAO. The tribological performance of the PAO 100 was enhanced dramatically by adding the HSNs. Antiwear and friction reduction mechanisms of nanoparticles as additives in lubricant are shown in *Figure 19*.

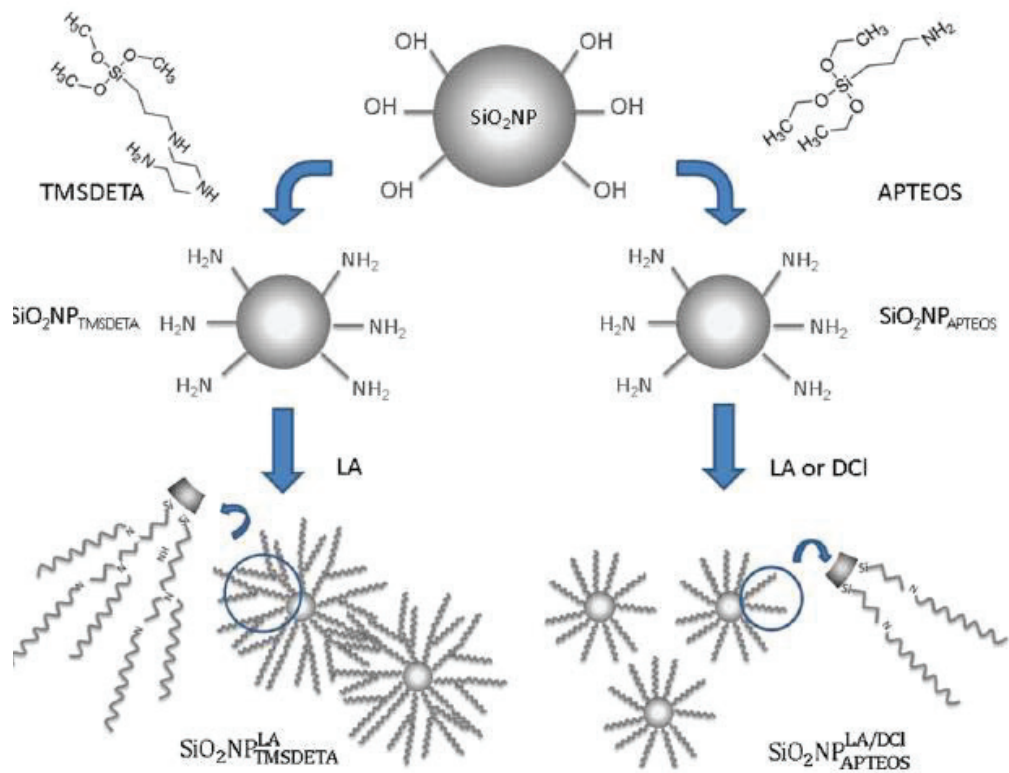


Figure 18 Sketch of the hybrid SiO<sub>2</sub> NPs functionalization (Source: Lopez et. al., 2015).<sup>36</sup>

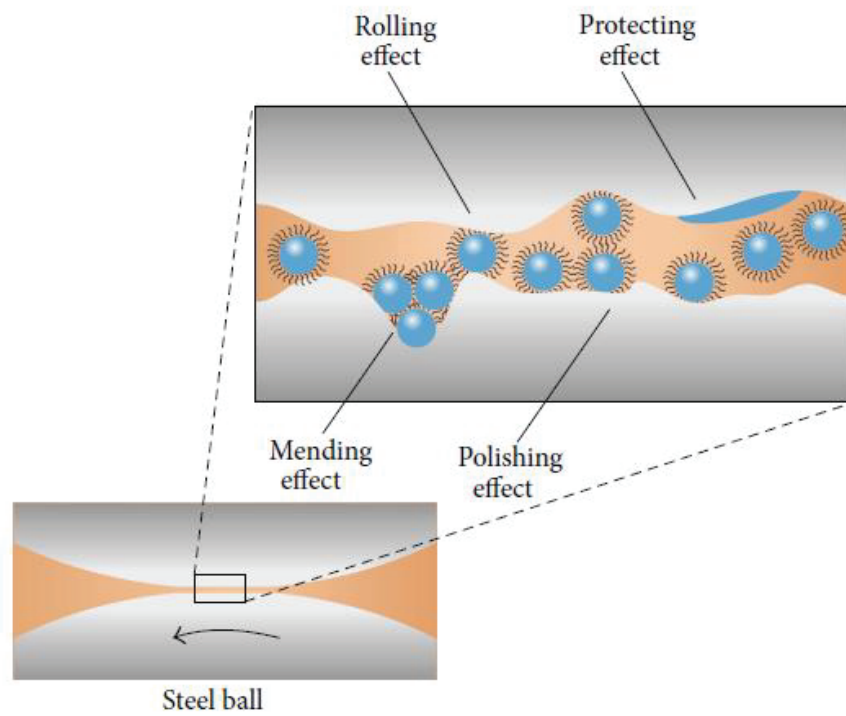


Figure 19 Schematic diagram of the lubrication mechanism of silica nanoparticle (Source: Sui et. al, 2015).<sup>37</sup>

When nanoparticles were taken into the contacting area by lubricants, they would fill asperities on the metal surface (mending effect) and polish the rough metal surfaces (polishing effect). Some nanoparticles can interact with the metal surface and form tribofilm, which could protect the surface and reduce the friction (protecting effect).

Since boron-based lubricants have shown multifunctional tribological behavior and silica nanoparticles could be modified easily, combination of them can be considered as potential replacements for phosphorus-, sulfur-, halogen-, and metal-containing lubricants.

## CHAPTER 3

### MATERIALS AND METHODS

Materials used for production, dispersion and analysis of composite nanoparticles are given in section 3.1. Second part covers all techniques to produce Si/Na-Borate composite nanoparticles, all methods for understanding the structure and morphology of them. Additionally, four ball test that used for evaluation of EP performance is explained succinctly.

#### 3.1. Materials

Tetraethyl orthosilicate (TEOS) (Merck, 98%) as silica source, ethanol (Tekkim, 96%) as solvent and ammonium hydroxide (NH<sub>4</sub>OH) (Sigma-Aldrich, 26%) as basic catalyst were used in the synthesis of SNPs. Ultrapure water (0.055 μS) was used in all the experiments. di-Sodium Tetraborate decahydrate (Na-Borate) (Na<sub>2</sub>B<sub>4</sub>O<sub>7</sub>\*10 H<sub>2</sub>O) (Merck, analysis grade) was used as boron source. Cetyl Trimethyl Ammonium Bromide (CTAB, Sigma-Aldrich) was used to disperse nanoparticles. Base oils were supplied from Opet Fuchs.

#### 3.2. Methods

In this chapter, methods to synthesize composite nanoparticles were stated. First of all, classical route for silica nanoparticle synthesis was explained and then modified version of this route that was developed for composite nanoparticle synthesis in this study was briefly interpreted. Furthermore, analysis techniques for using to understand structure, morphology and chemistry of composite nanoparticles were elucidated.



### 3.2.1. Synthesis and Characterization of Composite (Si/Na-Borate) Nanoparticles

For the synthesis of composite (Si/Na-Borate) nanoparticles, Stöber method, sol-gel synthesis route, was modified. Stöber process which is used for synthesizing spherical, monodisperse silica particles with different particle sizes ranging from 0.05 to 2  $\mu\text{m}$ .<sup>38</sup> The method is based on reaction of a silica source (tetraethyl orthosilicate, TEOS) with a water-ethanol mixture in the presence of an ammonium hydroxide ( $\text{NH}_4\text{OH}$ ) as a catalyst. The reactions in Stöber method are described as follows:<sup>39</sup>

Ionization of ammonia:  $\text{NH}_3 + \text{H}_2\text{O} \leftrightarrow \text{NH}_4^+ + \text{OH}^-$

Hydrolysis:  $\text{Si}(\text{OR})_4 + x\text{H}_2\text{O} \leftrightarrow (\text{OH})_x\text{Si}(\text{OR})_{4-x} + x\text{ROH}$

Alcohol condensation:  $\text{Si}(\text{OR})_4 + (\text{OH})\text{Si}(\text{OR})_3 \leftrightarrow (\text{OR})_3\text{Si}-\text{O}-\text{Si}(\text{OR})_3 + \text{ROH}$

Water condensation:  $(\text{OR})_3\text{Si}(\text{OH}) + (\text{HO})\text{Si}(\text{OR})_3 \leftrightarrow (\text{OR})_3\text{Si}-\text{O}-\text{Si}(\text{OR})_3 + \text{H}_2\text{O}$

R:  $\text{C}_2\text{H}_5$

In the classical Stöber method, the solution of ammonium hydroxide (1.09 M) and water (11.67 M) were mixed with ethanol (12.14 M) under mild stirring. Silica synthesis was done by the direct addition of TEOS (0.25 M). In the modified Stöber method used in this thesis study, sodium borate (Na-Borate, borax) solutions at different concentrations were prepared using distilled water. These Na-borate solutions were used instead of water in standard Stöber method. The molar ratios of other ingredients were kept constant. *Figure 20* illustrates the steps involved in the development of a silica network from TEOS.

The steps of the experimental procedure are listed and shown below (*Figure 21*).

- ✚ First of all, Na-Borate solution was prepared in distilled water at 50 °C, separately.
- ✚ Then, ammonium hydroxide was added to Na-Borate solution.
- ✚ After that, ethanol was measured and poured into reaction vessel.
- ✚ Next, TEOS was added to make reaction mixture.

- ✚ Reaction vessel was agitated with magnetic stirrer.
- ✚ Ammonium hydroxide/Na-Borate mixture was poured into a syringe and added (at a rate of 500 $\mu$ L/min) into reaction mixture that under mild agitation by using syringe pump.

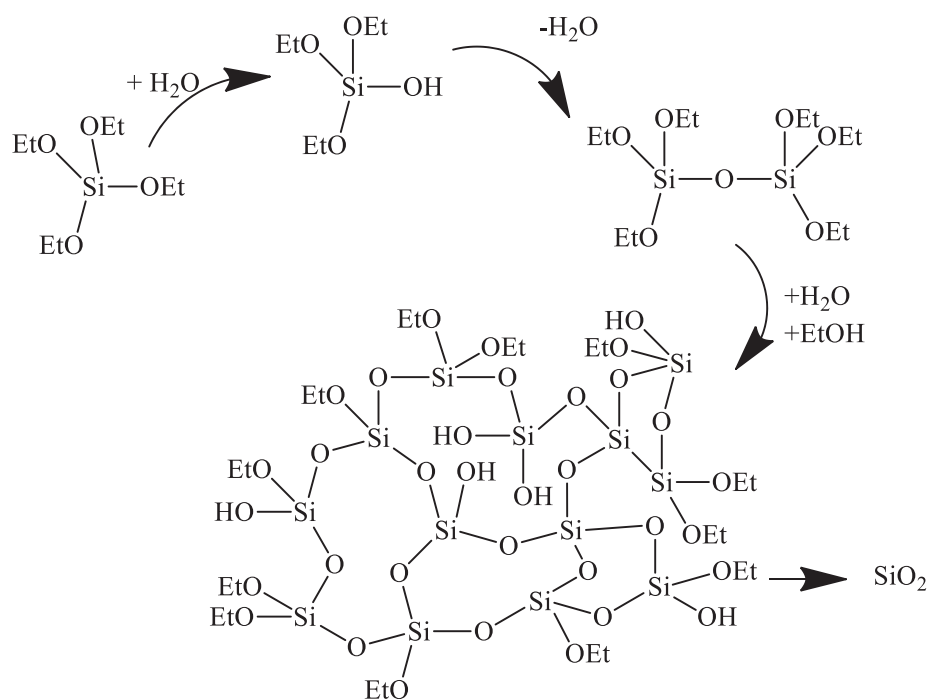


Figure 20 Silica network production through the hydrolysis and condensation reactions of TEOS (Source: Wikipedia).<sup>40</sup>

All the experiments were performed at room temperature ( $\sim 20^\circ\text{C}$ ) and reaction vessel were agitated during 24 hours for completion of the reaction. Reaction volumes were selected as 100 mL expect the material balance calculations. Representative samples were taken from the suspensions and size of particles were determined by SEM coupled by an image analysis software. Then, particles were separated from the solution using centrifugation and collected. The final particles were washed with water and ethanol to remove unreacted reagents. Finally, particles were dried at room temperature for characterization.

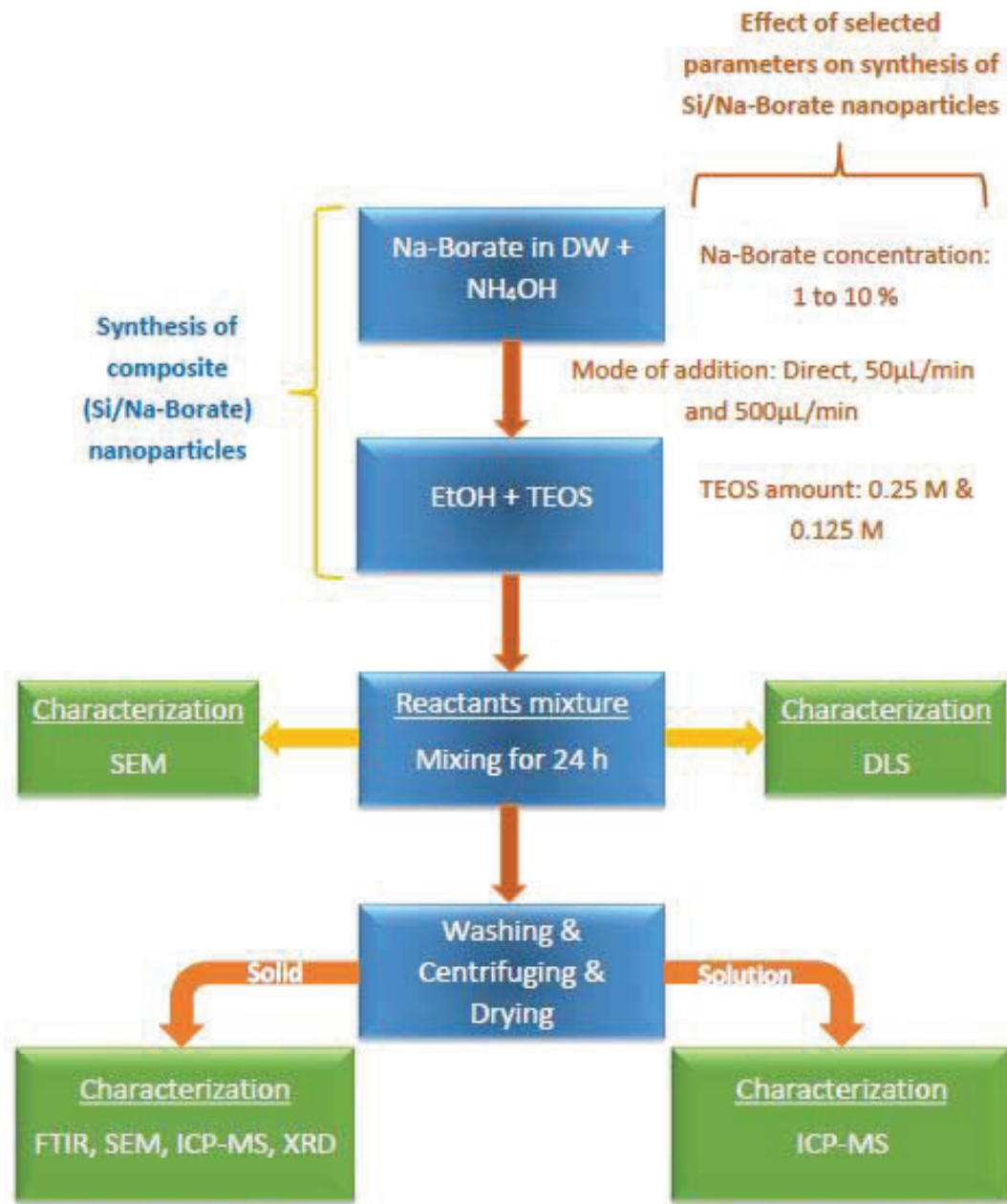


Figure 21 Composite (Si/Na-Borate) Silica Synthesis.

### 3.2.1.1. Effect of Na-Borate Concentration on Synthesis of Composite (Si/Na-Borate) Nanoparticles

The synthesis of Si/Na-Borate nanocomposite particles were performed at different concentrations of Na-Borate solution (from 1 to 10%) to clarify its effect on the morphology of particles. Na-Borate solubility in water at room temperature were limited to 4.7 % at 20 °C. Therefore, solutions were heated up to 50 °C exceed solubility limits (Figure 22). After reaction was done, the samples were collected and analyzed the morphology using SEM.

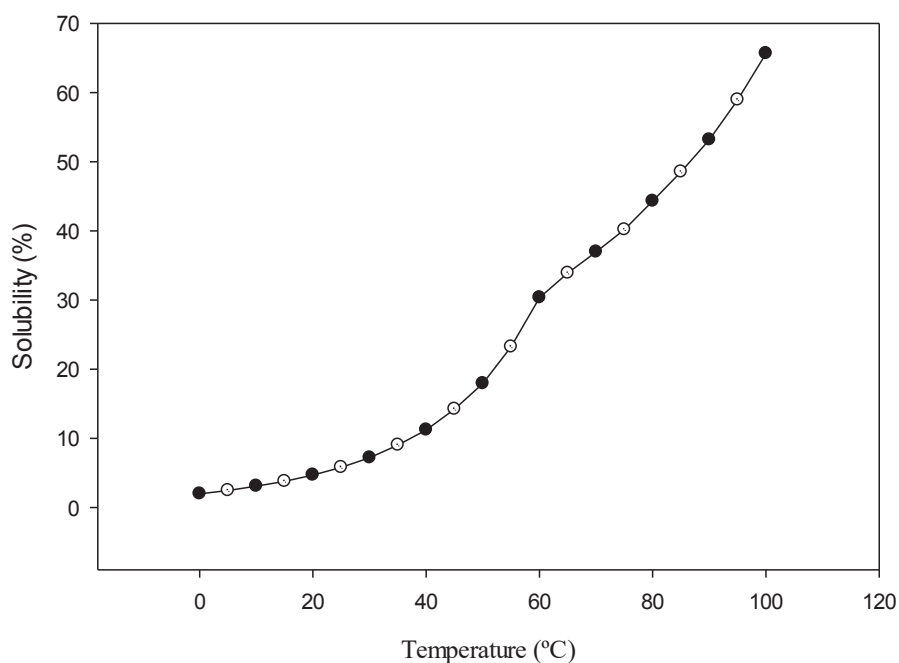


Figure 22 Solubility of Na-Borate in water at different temperatures.

### 3.2.1.2. Effect of TEOS amount on Synthesis of Composite (Si/Na-Borate) Nanoparticles

The synthesis of Si/Na-Borate nanocomposite particles were performed for 1%, 3% and 5% Na-Borate solution using two different TEOS amounts. One was the standard amount that is used for all the other experiments, the other was the half of the standard

amount. Addition rate of the ammonium hydroxide and borate solution mixture was 500  $\mu\text{L}/\text{min}$ . After the reactions were completed, SEM samples were collected to analyze the morphology of composite particles.

### **3.2.1.3. Effect of Mode of Na-Borate Addition on Synthesis of Composite (Si/Na-Borate) Nanoparticles**

The synthesis of Si/Na-Borate nanocomposite particles were performed using 5% Na-Borate solution and three different adding rates; direct addition, 500  $\mu\text{L}/\text{min}$  and 50  $\mu\text{L}/\text{min}$ . All experiments were done using the procedure given in the flowsheet. After 24h, SEM samples were collected. Then, particles were collected by centrifugation of the solutions and dried at 80 °C during 24h. Dried nanoparticles were weighted in order to calculate the number of particles.

### **3.2.1.4. Understanding the Structure of the Composite Nanoparticles**

The synthesis of Si/Na-Borate nanocomposite particles were performed using 5% Na-Borate solution by addition rate of 500  $\mu\text{L}/\text{min}$ . In these tests, a large reaction volume, 500mL, was used and the synthesis were repeated two times to keep the error at minimum. Then the suspensions were centrifuged and washed with ethanol. Both type of samples “washed” were collected for further analysis.

In order to investigate composite structure of the nanoparticles, distilled water in which boron is soluble and silica is not soluble was used. 0.1 g of composite nanoparticle that synthesized with 5% Na-borate solution were dispersed in 10 ml DW. Ultrasonic probe was used for dispersion of the particles and waited 24 hours for the dissolution of Na-borate. Then, samples were centrifuged in order to separate solvent phase. Next, particles were washed with ethanol three times and kept in room temperature to dry. Samples of solvent was collected to analyze by using ICP-MS and SEM in comparison with original particles that is not treated.

### **3.2.1.5. Material Balance**

In order to make material balance calculations for boron element, this procedure was followed.

- ❖ 0.1 g of composite nanoparticles synthesized with 5% Na-borate solution were dispersed in 10 ml DW.
- ❖ Ultrasonic probe was used for dispersion of the particles and dissolution of Na-borate was achieved in 24 hours.
- ❖ Samples were centrifuged to separate the solvent phase.
- ❖ Solid phase was decomposed using wet digestion method (3 M HCl & 1 M HNO<sub>3</sub>)
- ❖ ICP-MS, XRD and FTIR was used for analysis

### **3.2.2. Tribological Performance of Composite Nanoparticles**

In this chapter, dispersibility of nanoparticles in various medium was studied firstly. After getting the stable systems, performance tests were done with using Four Ball Tester (*Figure 23*) by Opet Fuchs.

#### **3.2.2.1. Dispersion of Composite Nanoparticles**

Five different base oils generally use in lubricant formulations. Structure of the base oils are listed below.

- Base Oil-1 is a kind of mineral oil,
- Base Oil-2 is a refined mineral oil that has a lower Sulphur (S) content,
- Base Oil-3 and Base Oil-5 are synthetic oils,
- and Base Oil-4 is a synthetic polyolefin.

Base oil 1 (mineral oil) was used as continuous phase. The dispersion of Silica/Na-Borate particles were achieved through use of an ultrasonic probe in the presence of CTAB (cationic surfactant).

### **3.2.2.2. Four Ball Extreme Pressure Test to define the Load-Wear Index and Weld Point**

This test method involves determining the load-wear index and welding load of lubricating oils and determining the load-bearing capacity of the lubricant.

In the fixed horizontal plane, the three steel balls covered by the lubricant with a temperature of 18-35 °C are rotated for 17 seconds at  $1760 \pm 40$  rpm by an another ball, which has similar properties like the other balls, that is rotated by a spindle moving from the engine and under certain load for 10 seconds (*Figure 24*).

This process is continued until the applied load is increased and the four balls are welded (*Figure 25*) to each other and the load at this moment is recorded as the boiling load of the lubricant.

The diameters of the abrasions (*Figure 25*) occurring in the balls in each test until the boiling load is determined are measured by a microscope and the load-wear index of the lubricant is calculated with the help of the correlations in the test method.



Figure 23 Four Ball Tester (Source: Koehler Instrument).<sup>41</sup>

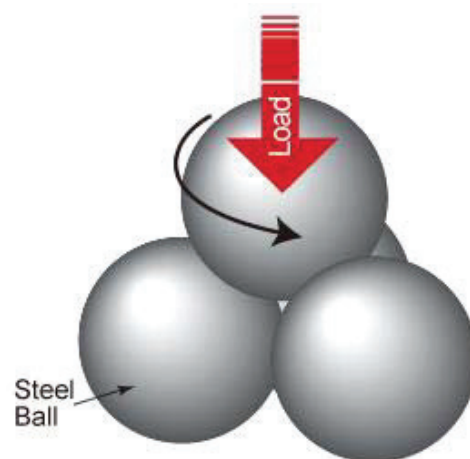


Figure 24 Rotated steel balls in the Four Ball Tester (Source: Sumico Company).<sup>42</sup>



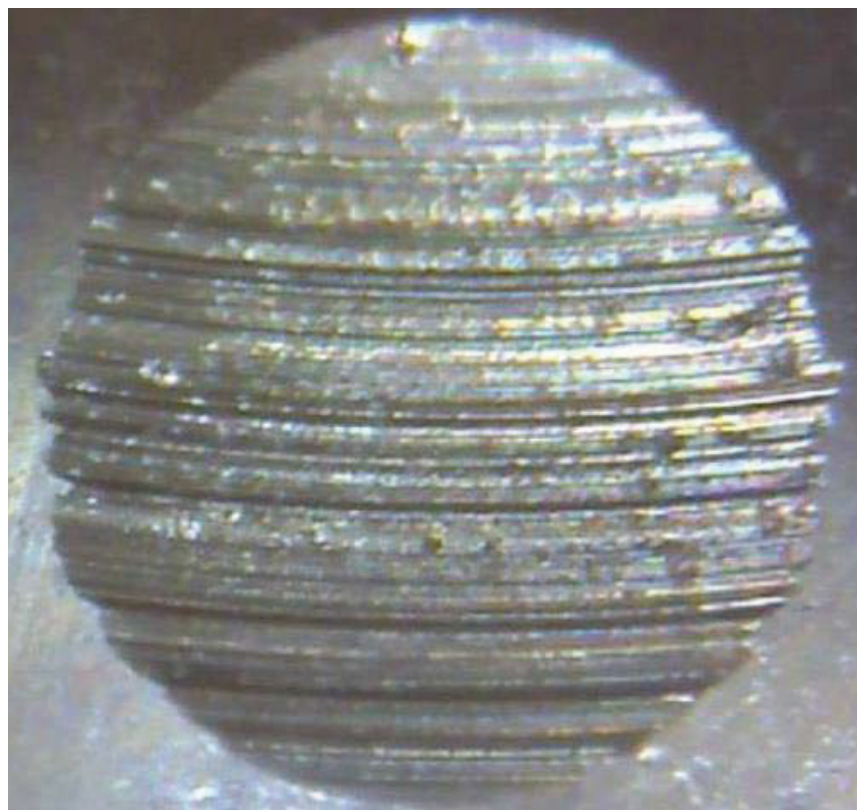


Figure 25 Welded balls (left), abrasions on the surface of the ball (right)  
(Source: Ducom Material Characterization systems).<sup>43</sup>

## CHAPTER 4

### RESULTS and DISCUSSIONS

The results of the studies conducted in this thesis were discussed in the following paragraphs. Details of these experiments were previously discussed in Chapter 3. First part of the study contains the synthesis and characterization of composite nanoparticles. Second part contains the studies for dispersion of nanoparticles in an oil phase and the tests for the performance of these composite nanoparticles in oil phase.

The morphology of these composite nanoparticles were characterized by SEM. Size distributions of these particles were obtained using SEM images. The chemical structures of nanoparticles were determined by ICP-MS, XRD and FTIR analysis. Zeta potential and size measurements were done using DLS instrument.

#### 4.1. Synthesis and Characterization of Composite (Si/Na-Borate) Nanoparticles

In Stöber synthesis, silica was formed in ethanol-water mixture in the presence of catalyst ammonia. In the unmodified case, TEOS was dissolved in ethanol and reaction was initiated by adding water-ammonia solution into ethanol mixture. TEOS went into hydrolysis and condensation reactions producing three to four hundred nm perfectly spherical particles (*Figure 27–A*). First, Na-borate was gradually added to the ethanol and large pure borate crystals were observed (*Figure 27–B*). Basically the difference between two was the presence of TEOS in the case of A. Then, Na-Borate was added directly (Pulse addition) into an ethanol solution that already have silica particles obtained using Stöber method. The SEM pictures obtained this way was presented in *Figure 27-C*. As seen from the figure that Na-Borate creates large crystals on side of silica particles. These particles attach on the surfaces of borate crystals. So, it is clear that sodium borate does not precipitate around pre-formed silica nanoparticles. The zeta potential results are given in *Figure 26*. These results show that the negatively charged silica nanoparticles may stick on zero charged borate crystals.

Then, sodium borate was added gradually into an ethanol solution using microsyringe in order to create small crystals to go on to the surface of the silica particles and create a Na-Borate shell around the silica particles (*Figure 27–D9*). It is seen from the figure that even larger Na-Borate crystals were formed and silica nanoparticles were embedded in these crystals.

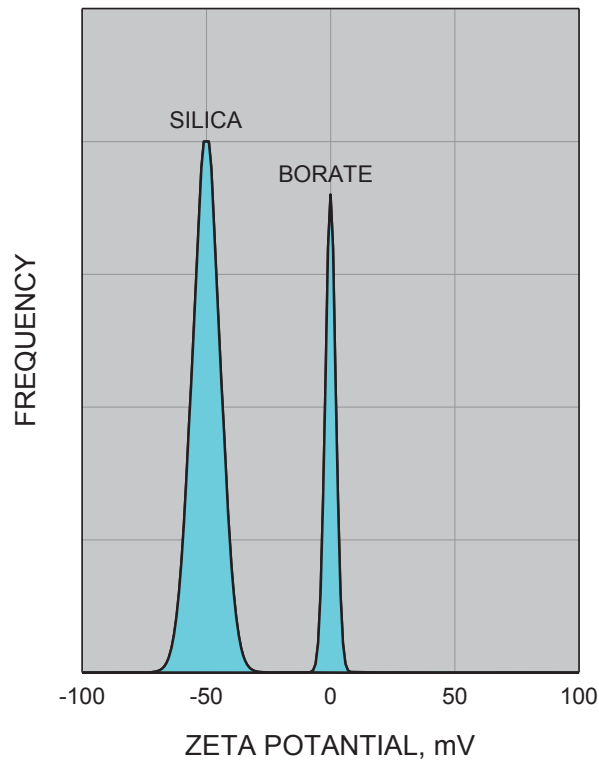


Figure 26 Zeta potential measurements of pure silica and Na-Borate.

As summary, our findings show that:

- ✓ Na-Borate precipitates as separate crystalline phase when added directly to ethanol-water solution.
- ✓ Na-Borate again precipitates as separate crystalline phase when added directly to ethanol-water solution containing amorphous silica nano particles as seeds and these particles adhere on the Na-Borate crystals.
- ✓ Gradual addition of Na-Borate does not prevent crystal formation but lead to the formation of silica particles embedded Na-Borate crystals.

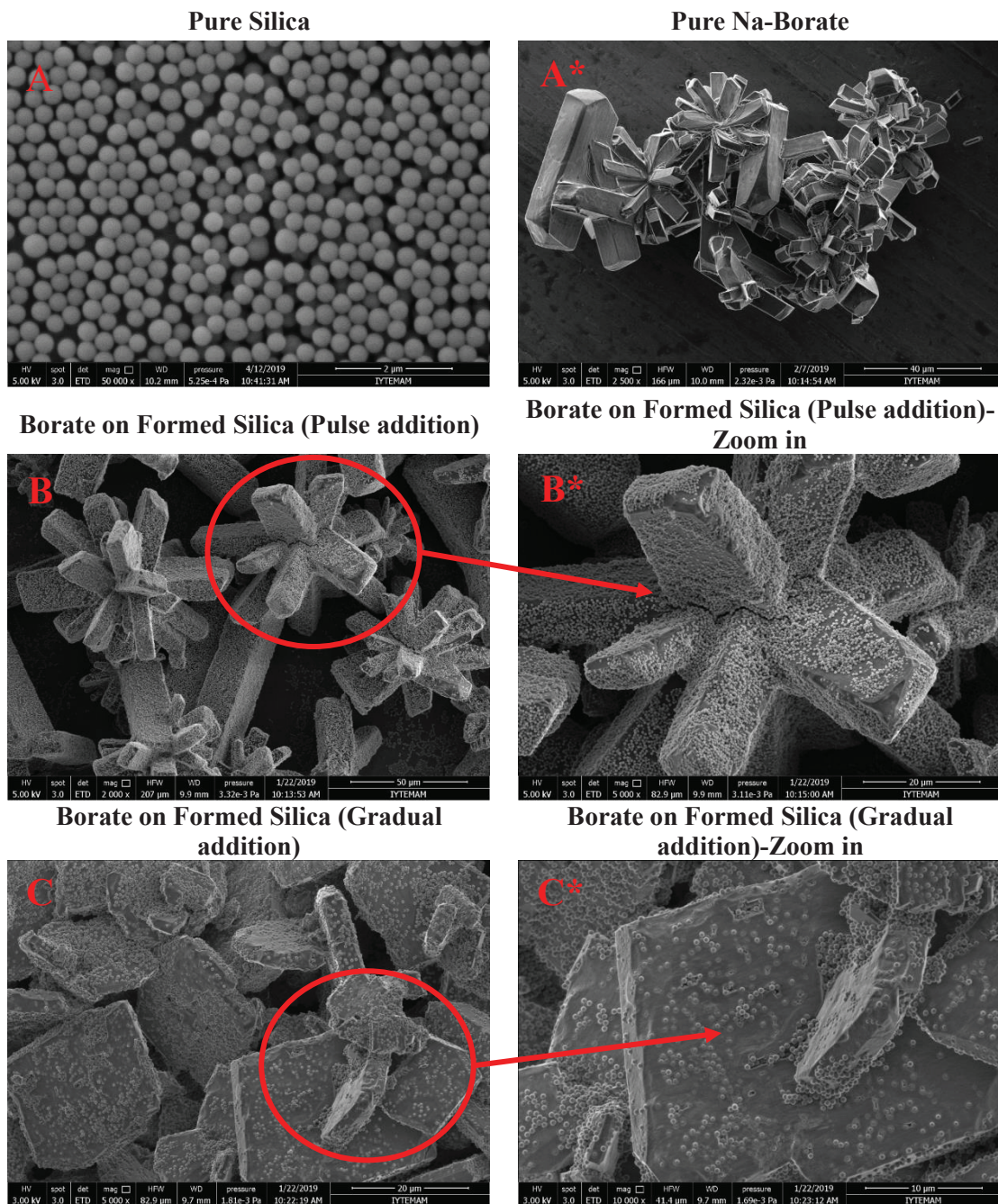


Figure 27 Progress of forming composite Silica/Na-Borate nanoparticles.

However, when Na-Borate is added gradually into an ethanol solution in the presence of TEOS, Borate and silica nanoparticles co-precipitate in the form of amorphous composite spherical particles (Figure 28-B). The synthesis of these particles, Silica/Na-borate composite nanoparticles, were conducted under different conditions and discussed in the following sections. For this purpose, the effect of;

- The amount of Na-borate,
- The rate of ammonium hydroxide and Na-Borate solution mixture addition,
- The amount of TEOS on the particle size distribution and shapes (morphology) of the nanoparticles were investigated.

#### **4.1.1. Effect of Na-Borate Concentration on Synthesis of Composite (Si/Na-Borate) Nanoparticles**

To test the effect of Na-borate concentration on the particle size and shape of the nanocomposites, the modified Stöber synthesis was done at different concentrations of Na-Borate solutions from 0% to 10% while all other ingredients were kept constant. SEM images of these particles were presented in *Figure 29*. It is clearly seen that, the size of composite nanoparticles varies with increasing concentration of Na-Borate. After 1%, the agglomerated structures start to form.

As mentioned before, perfectly spherical silica nanoparticles were obtained by modified Stöber method (*Figure 28-A*). When our new procedure were applied that means Na-Borate (1% solution) and ammonia gradually added into ethanol-TEOS mixture, perfectly spherical but large nanoparticles were obtained (*Figure 28-B*). So, it is clearly seen that Na-borate is in the structure of silica particles. That is, larger composite nanoparticles were obtained.

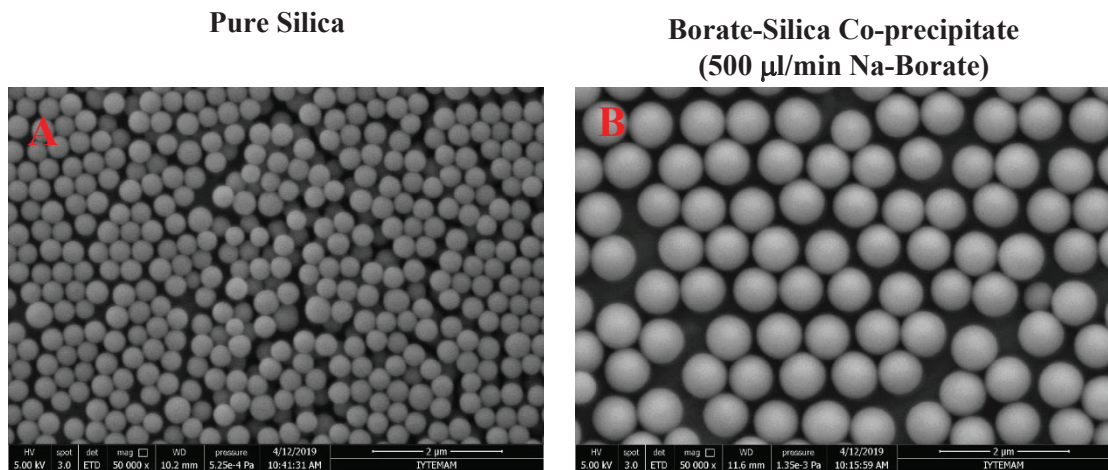


Figure 28 Difference between Si/Na-Borate composite nanoparticles and pure silica nanoparticles.

#### 4.1.2. Effect of Na-Borate Concentration on the Chemical Structure of Composite Nanoparticles

To analyze the chemical structure of composite nanoparticles, ICP-MS, XRD and FTIR were used.

Based on the XRD analysis, one can say that:

- ✓ Amorphous silica gives a broad peak at  $2\theta$  of  $22^\circ$
- ✓ Amorphous Na-Borate gives a broad peak at  $2\theta$  of  $25^\circ$
- ✓ Manufactured amorphous Silica/Na-Borate particles gave a broad peak at  $25^\circ$ .

The XRD results of composite nanoparticles were given in Figure 30. We know that Na-Borate is in crystalline structure naturally. Difference between the characteristic XRD peaks were seen in *Figure 30*. Amorphous borate gave a broad peak at  $25^\circ$ . On the other hand, amorphous silica nanoparticles gave a different broad peak at  $22^\circ$ . Hence, composite nanoparticles gave a broad peak at around  $25^\circ$  and had amorphous structure.

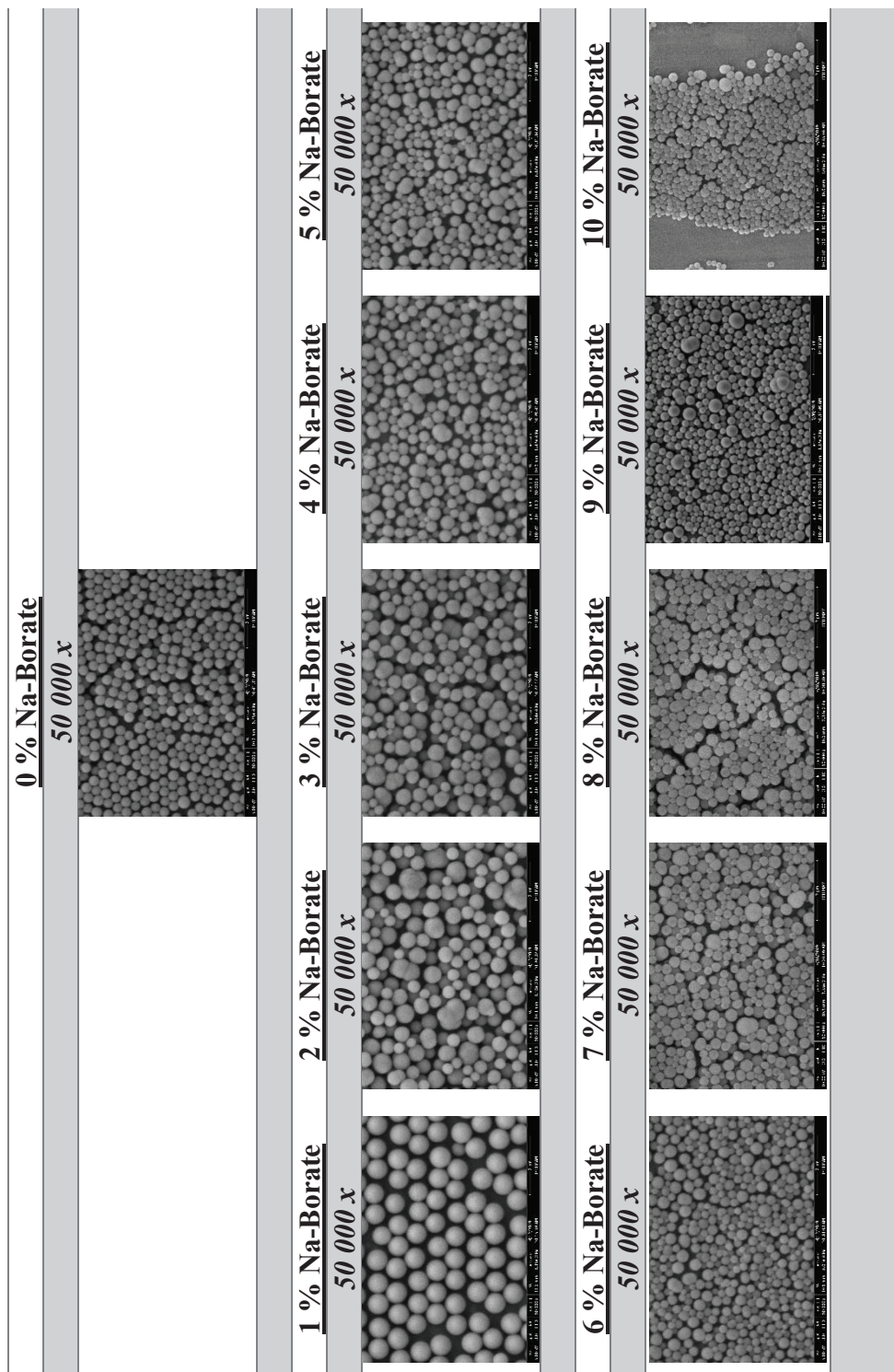


Figure 29 SEM pictures of composite nanoparticles contain 1 to 10% Na-Borate in comparison with neat silica particles.

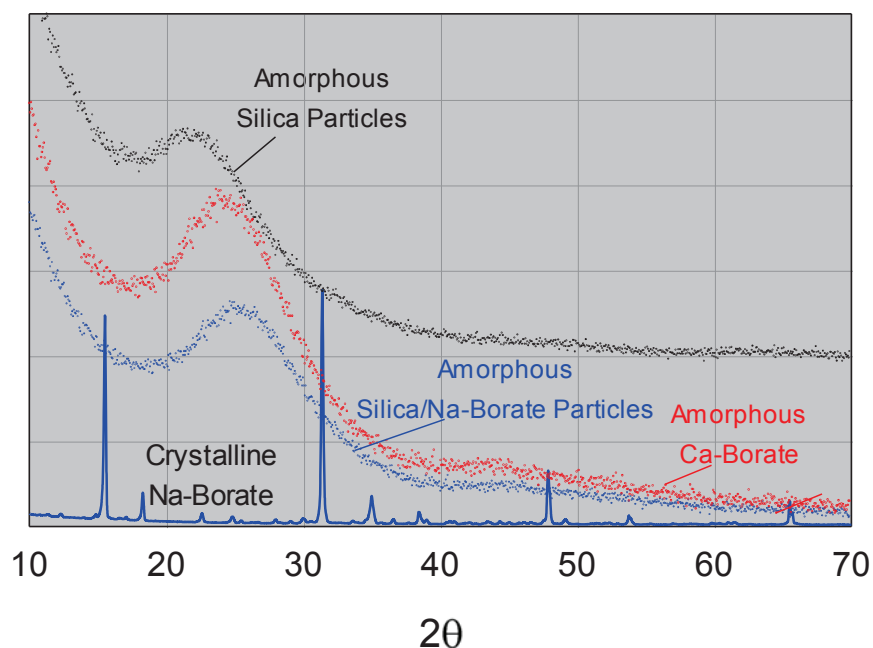


Figure 30 XRD results of composite nanoparticles.

ICP-MS was used to determine the amount of boron left in supernatant after centrifugation and separation of solid particles from the suspension. These results were presented in *Table 10*.

Table 10 ICP-MS results of composite nanoparticles

Na-Borate $\text{Na}_2\text{B}_4\text{O}_7 \cdot 10\text{H}_2\text{O}$ (%)	Na-Borate $\text{Na}_2\text{B}_4\text{O}_7 \cdot 10\text{H}_2\text{O}$ (g)	B initial in solution (g)	B residual in supernatant ( $\text{g} \times 10^{-3}$ )	B in particles (g)	B in solid form (%)
1	1.08	0.122	ND	0.122	100.0
3	3.24	0.367	0.597	0.366	99.8
3	3.24	0.367	9.629	0.357	97.4
5	5.40	0.612	12.910	0.599	97.9
5	5.40	0.612	22.140	0.590	96.4

Where,  $B_{(0)}$  is the initial concentration of boron before the reaction. B is the final concentration in the mixture after the separation of solid nanoparticles. Based on these results, almost all Na-Borate was fixed in the structure of composite nanoparticles.

FTIR analysis was also performed for solid part of the reaction mixture and chemical composition of the composite nanoparticles were compared with neat silica nanoparticles and Na-Borate powder.



As seen in *Figure 31*, *Figure 32*, *Figure 33* and *Figure 34*, important characteristic peaks were colored.

- (a) Red indicates the Si-O-Si bond,
- (b) blue indicates the  $\text{BO}_3$  bond,
- (c) green indicates the Si-O bond and
- (d) purple indicates the Si-OH bond.

According to the figures, it is clearly sees that;

- (a) Characteristic bulk Si-O-Si peak decreasing and shifting,
- (b) Characteristic  $\text{BO}_3$  borate peak increasing,
- (c) Characteristic surface Si-O peak decreasing, and
- (d) Si-OH peak disappearing for composite nanoparticles.

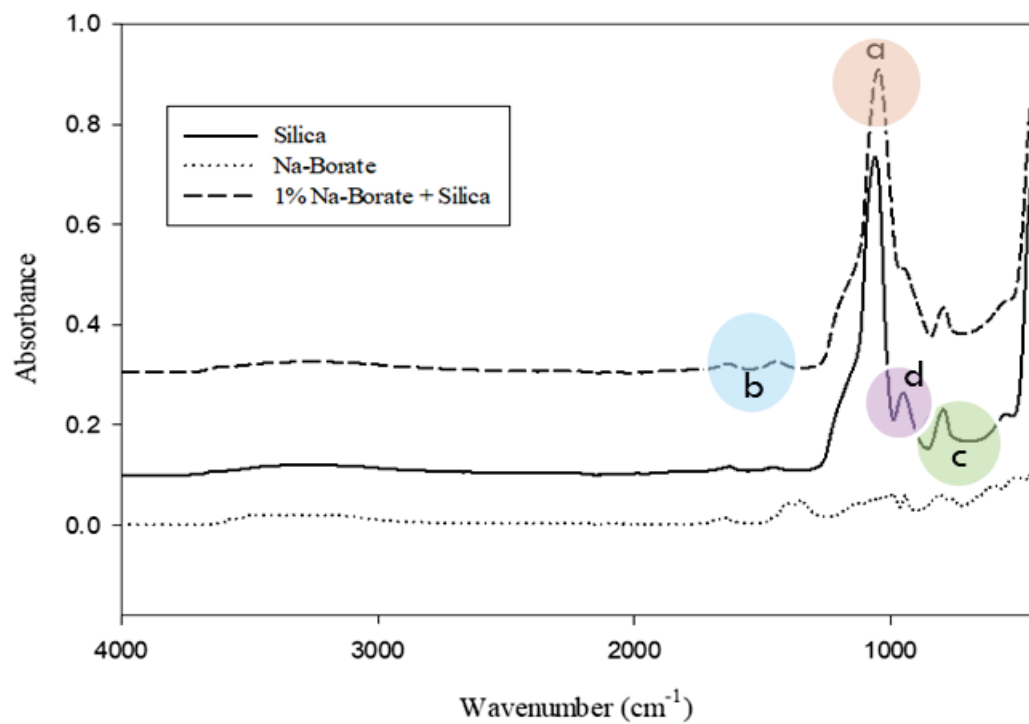


Figure 31 FTIR analysis result of composite nanoparticle with 1% Na-Borate.

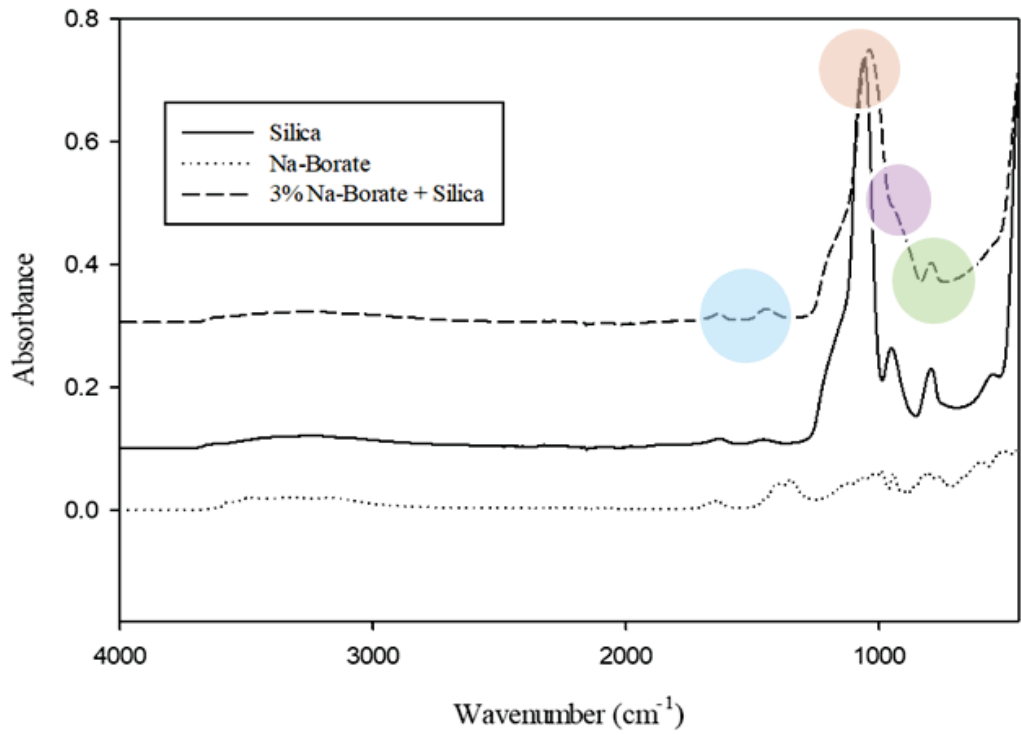


Figure 32 FTIR analysis result of composite nanoparticle with 3% Na-Borate.

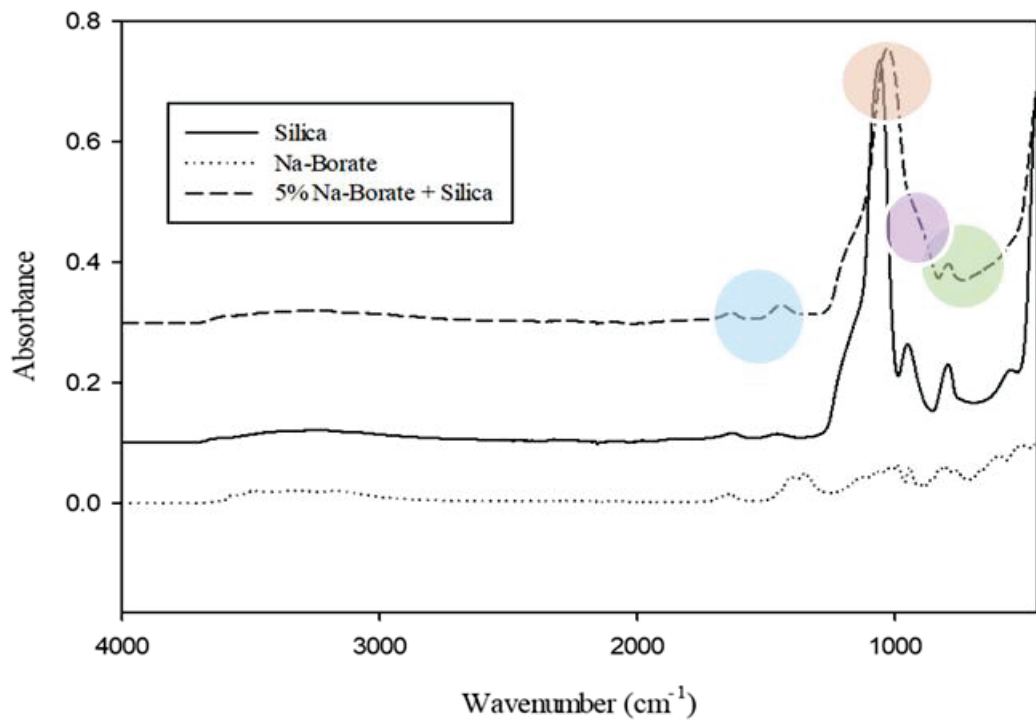


Figure 33 FTIR analysis result of composite nanoparticle with 5% Na-Borate.

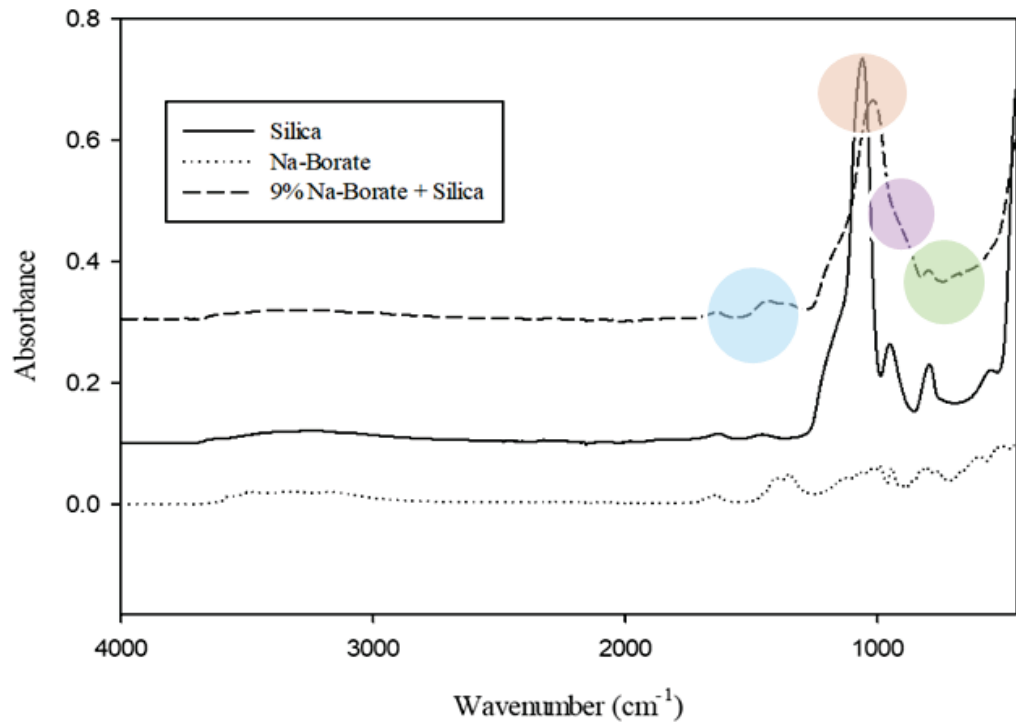


Figure 34 FTIR analysis result of composite nanoparticle with 9% Na-Borate.

The band at  $1341\text{ cm}^{-1}$  assigned to asymmetric stretching vibrations of trihedral ( $\text{BO}_3$ ) groups appeared on the spectra of composite nanoparticles at the beginning and increased slightly with increasing Na-Borate concentration. On the other hand, asymmetric vibration of Si-O ( $1090\text{ cm}^{-1}$ ) and symmetric vibration of Si-O ( $815\text{ cm}^{-1}$ ) appeared at the beginning and decreased as borate concentration increased. This might be mean that borates was reacted with Si-O groups of silica nanoparticles.

Additionally, peaks at around the  $1000\text{ cm}^{-1}$  was shifted to the lower wave number side in composite nanoparticle spectrum. It was probably the proof of silica-boron interaction (most probably H-bonding). Because, if masses of involved atoms increase, peak could be shift to lower wavenumbers. The extent of frequency shift was often directly correlated with level of specific molecular interactions, such as hydrogen bonding interactions.

So, based on the results discussed, the following conclusions can be make:

- ✓ Size of the composite particles varied with increasing Na-Borate concentration.

- ✓ Almost all Na-Borate in solution was fixed in the structure of the composite particles up to 5% Na-Borate.
- ✓ Excess Na-Borate above 5% precipitated around composite particles as a separate phase cementing the individual particles.

#### **4.1.3. Effect of TEOS Concentration on the Chemical Structure of Composite Nanoparticles**

Effect of TEOS concentration on the morphology and chemical structure of composite nanoparticles were investigated and SEM images of these particles were presented in the following *Figure 35*. It is clearly seen that, at high Na-Borate/TEOS ratio, excess Na-Borate cemented the composite particles. The particles size distributions and the shape of particles, on the other hand, look very similar.

#### **4.1.4. Effect of Mode of Na-Borate Addition on Synthesis of Composite (Si/Na-Borate) Nanoparticles**

Three different addition modes (direct addition, 500  $\mu\text{L}/\text{min}$ , and 50 $\mu\text{L}/\text{min}$ ) of Na-Borate (for 5% Na-Borate solution) were performed to test the effect of Na-Borate addition rate on morphology of composite nanoparticles. SEM images of these particles are given in *Figure 36*. At high addition rate, excess Na-Borate precipitated separately and cemented the composite particles. In the case of direct addition, there are small and large particles and large particles are filled with small ones. The small ones seem like silica particles, the large ones seem like borate particles. They form as separate particles not composite particles. In the case of 50  $\mu\text{L}/\text{min}$  per minute, on the other hand, the particles are very small and agglomerated and seem that the particles cannot grow. This effect of sodium ion in Na-borate on silica growth is very similar to the effect of ions on the silica growth. The presence ions depress the electrical double layer around the particles and cause an agglomeration between particles when they are really small.

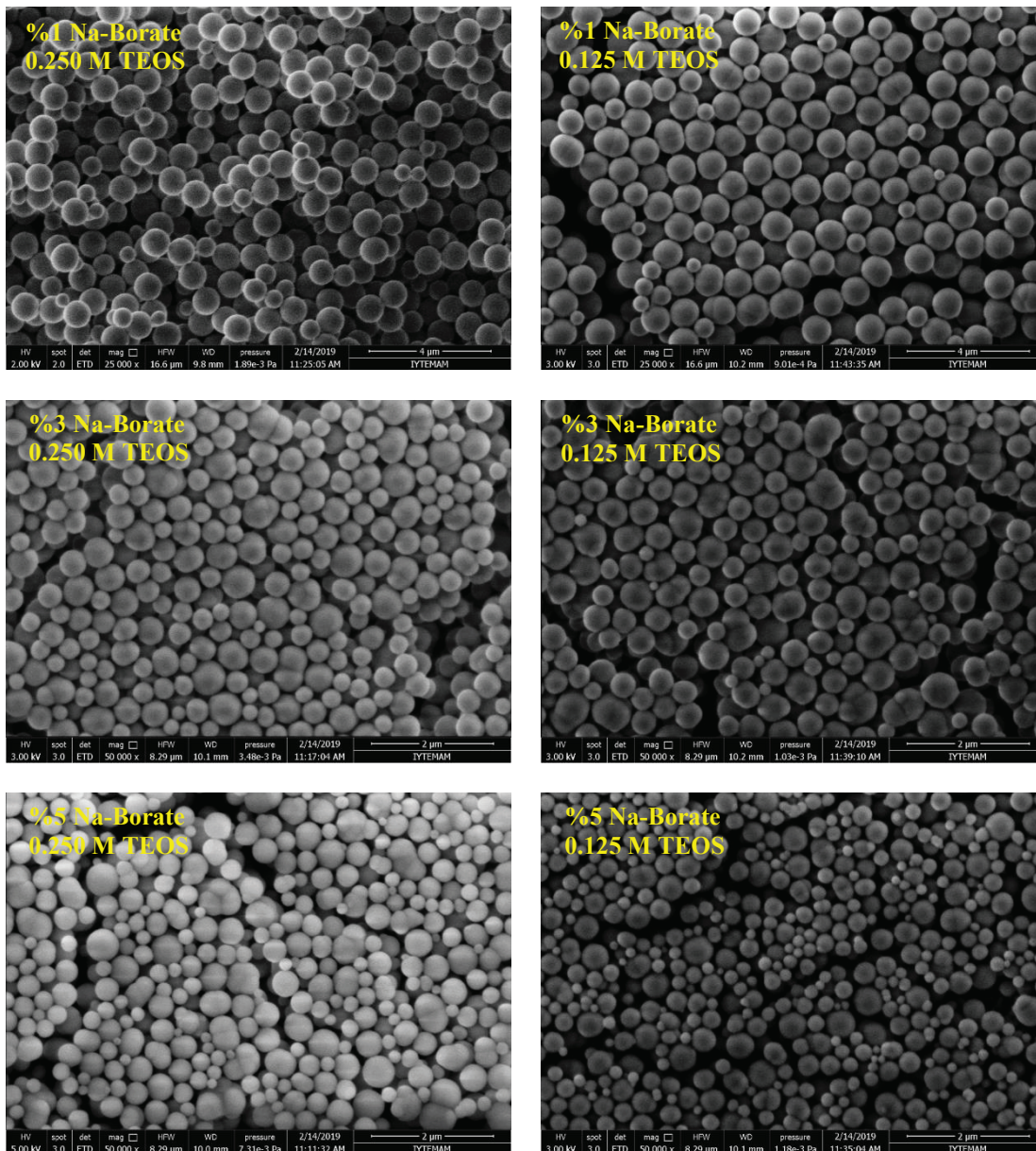


Figure 35 SEM pictures of nanoparticles contain 1%, 3% and 5% Na-Borate, effect of TEOS amount.

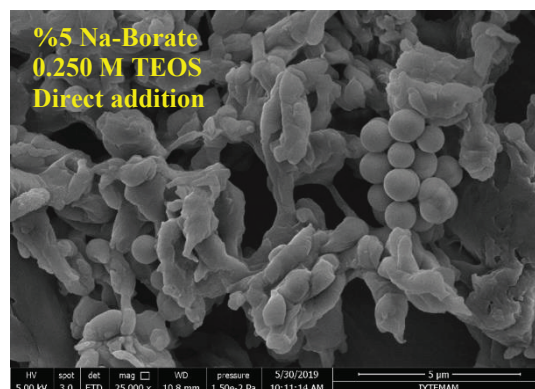
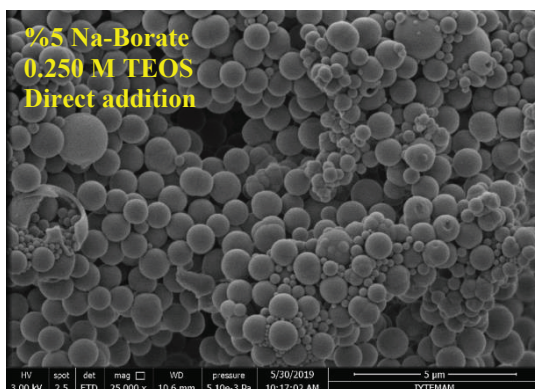
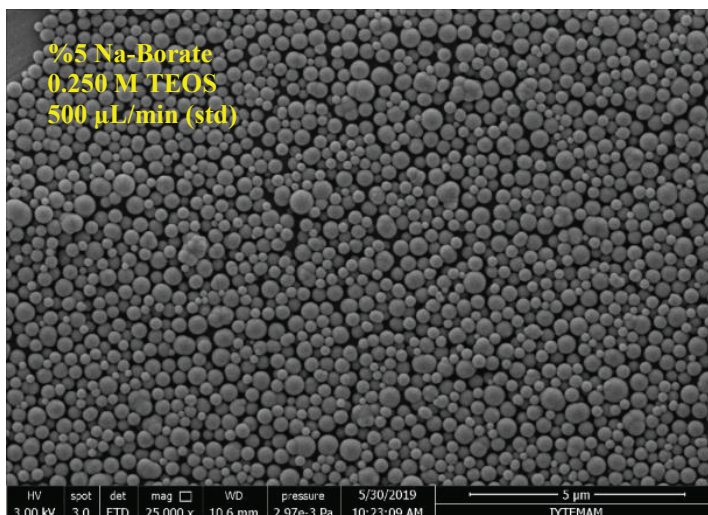
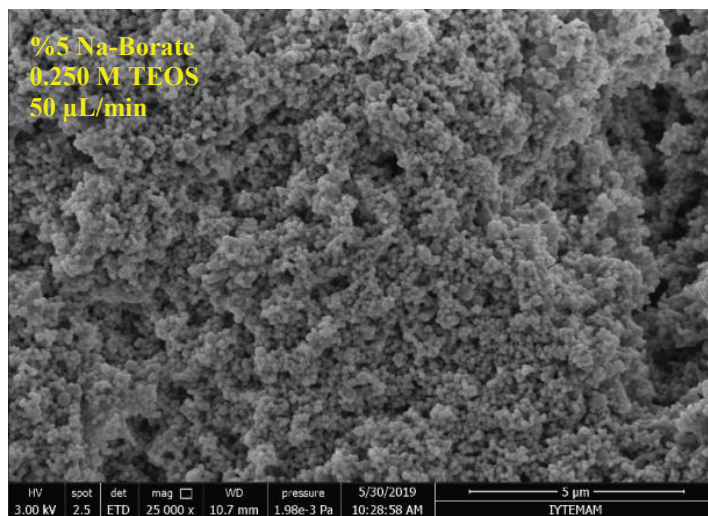


Figure 36 SEM pictures of nanoparticles that contain 5% Na-Borate synthesized with addition rate of direct, 500 $\mu$ L/min and 50 $\mu$ L/min.

#### 4.1.5. Understanding the Structure of the Composite Nanoparticles

To characterize the chemical structure of composite nanoparticles indeed to identify the Si and B parts of the particles, some tests were conducted using both ICP-MS and FTIR. This way one can identify the chemical structure of the particles whether they (Si and B) form together in one particle or they form as separate parts in particle. First of all, the reproducibility of the particles produced were tested. For this purpose, two parallel particle synthesis experiments were performed and characterized using SEM images (*Figure 37*).

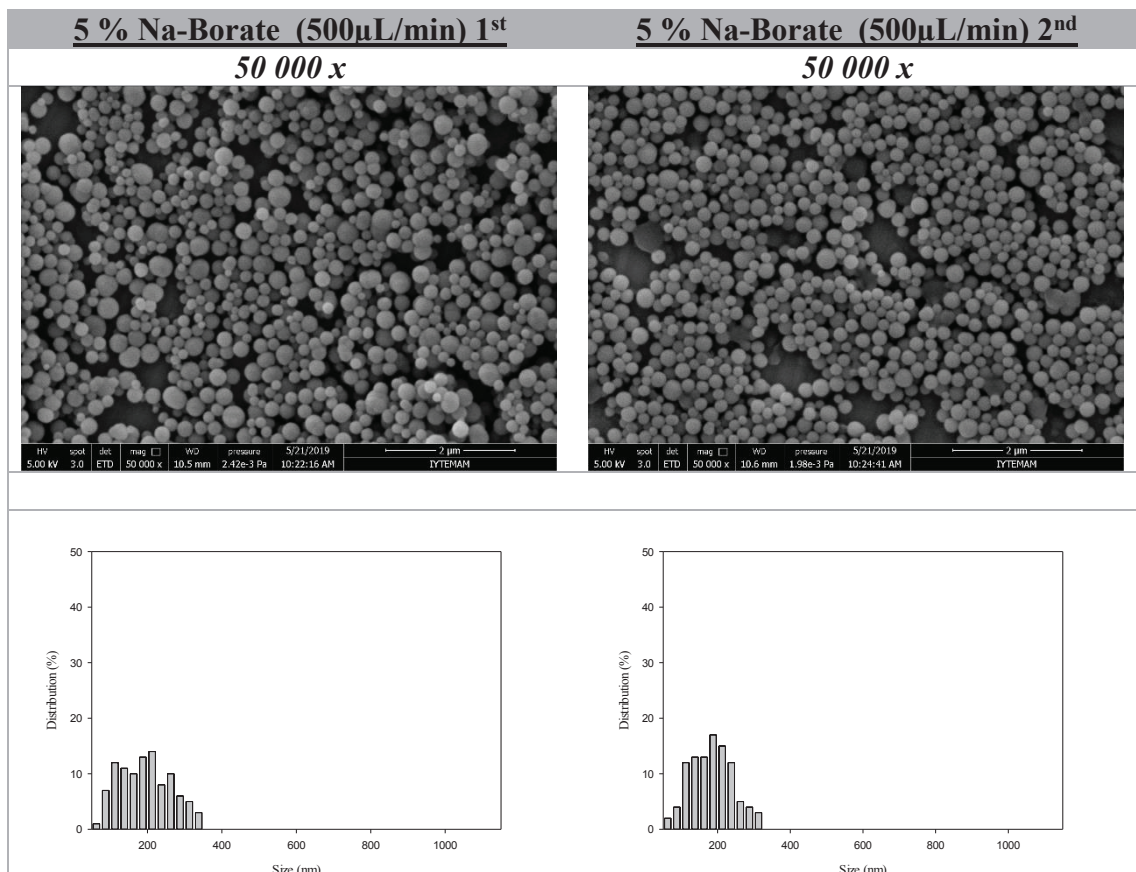


Figure 37 SEM pictures and size distributions of nanoparticles that contain 5% Na-Borate synthesized for repeatability test.

As seen from the SEM images, particle size distributions of both experiments are so similar. This shows that new method used for production of composite nanoparticles give reproducible results.

Some tests were carried out to understand the composite chemical structure of the nanoparticles. For this purpose, composite particles were dissolved in distilled water in which boron is soluble and silica is not. Then, samples were analyzed by SEM, ICP-MS and presented in *Figure 38* and *Table 11*.

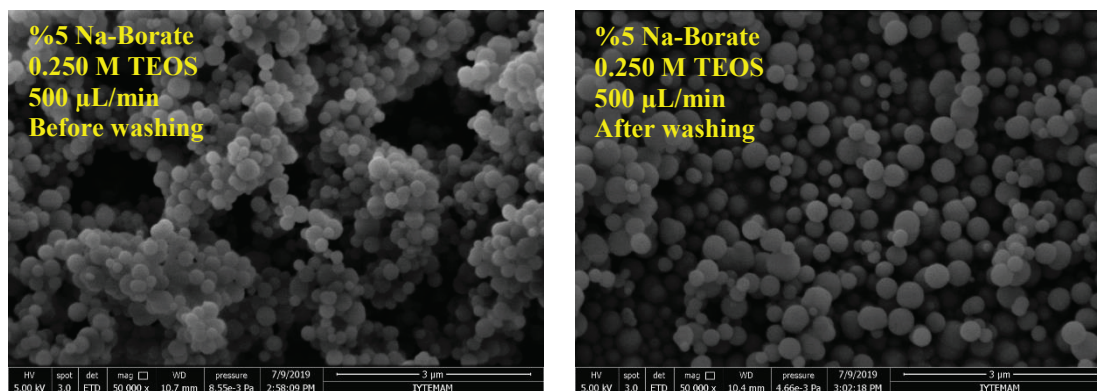


Figure 38 Effect of simple washing on morphology of composite nanoparticles.

Table 11 ICP-MS results of simple washing test

Na-Borate Na <sub>2</sub> B <sub>4</sub> O <sub>7</sub> ·10H <sub>2</sub> O (%)	Na-Borate Na <sub>2</sub> B <sub>4</sub> O <sub>7</sub> ·10H <sub>2</sub> O (g)	B initial in solution (g)	B residual in supernatant (g x10 <sup>-3</sup> )	B in particles (g)	B in solid form (%)
5	5.40	0.612	195.3	0.417	68.1

It is obvious that, the separate phase of Na-Borate was removed easily after simple washing with water. But, nearly 70% of boron still remained in the structure. This might be because of H-bonding of tetraborate ions [B(OH)<sub>4</sub>]<sup>-</sup> that are present at high pH in solutions, with silicon readily. It is known that, Na-Borate molecules are converted to tetraborate ion at higher PH levels as seen in *Figure 39*. In these case, Na-Borate molecules are expected to hydrolyze to tetraborate ions [B(OH)<sub>4</sub>]<sup>-</sup> at high pH values.

The gradual addition of Na-Borate co-precipitated with silica in the form of amorphous composite spherical particles when synthesized in the presence of sufficient amount of TEOS (*Figure 40*). At high Na-Borate/TEOS ratio or addition rate, excess tetraborate precipitated as a separate Na-Borate phase, cementing the composite particles (*Figure 41*). The presence of a separate Na-Borate phase could be substantiated by its removal through simple washing (*Figure 38*).



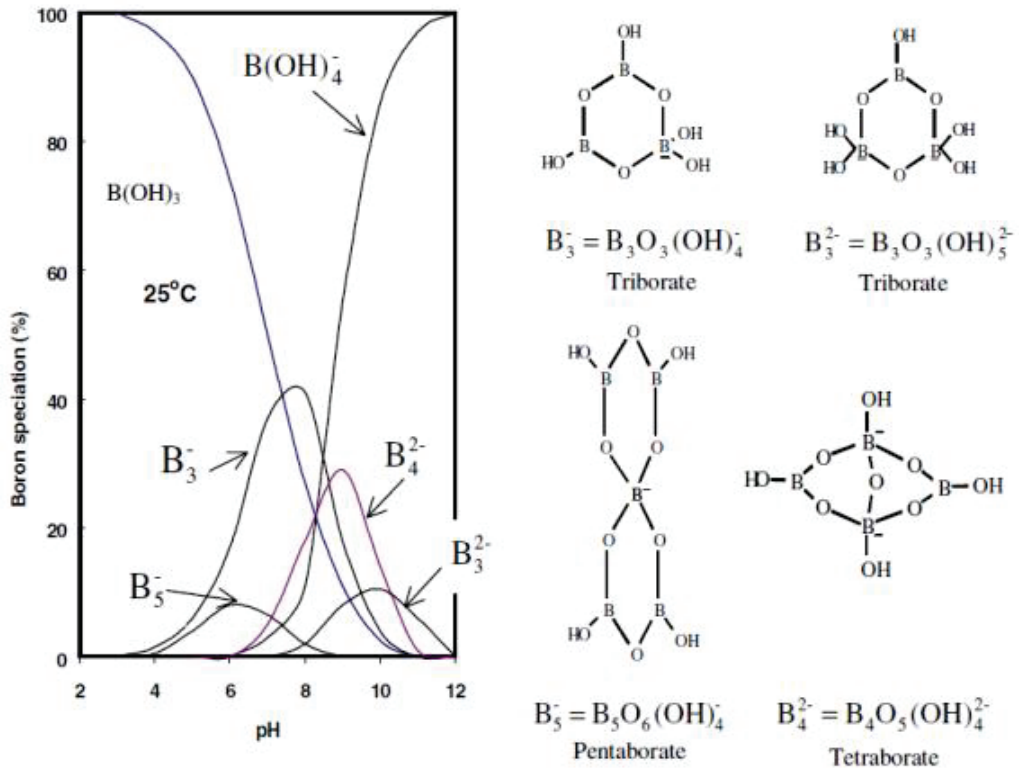


Figure 39 Borate ions at different pH levels (Source: Theiss et. al., 2013).<sup>44</sup>

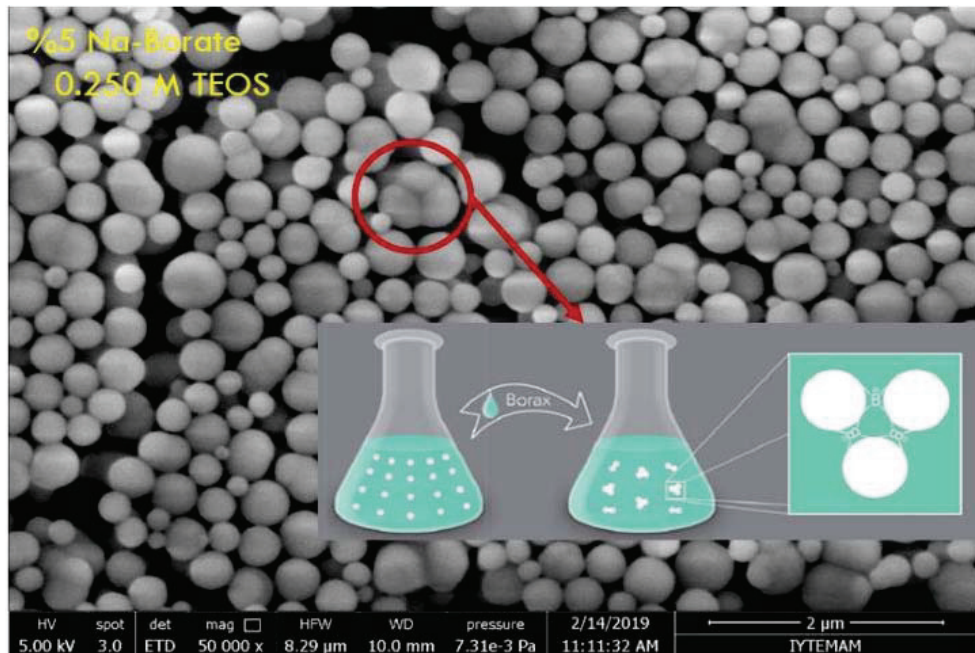


Figure 40 Literature example of precipitate structure (Source: Geng et. al., 2017).<sup>45</sup>

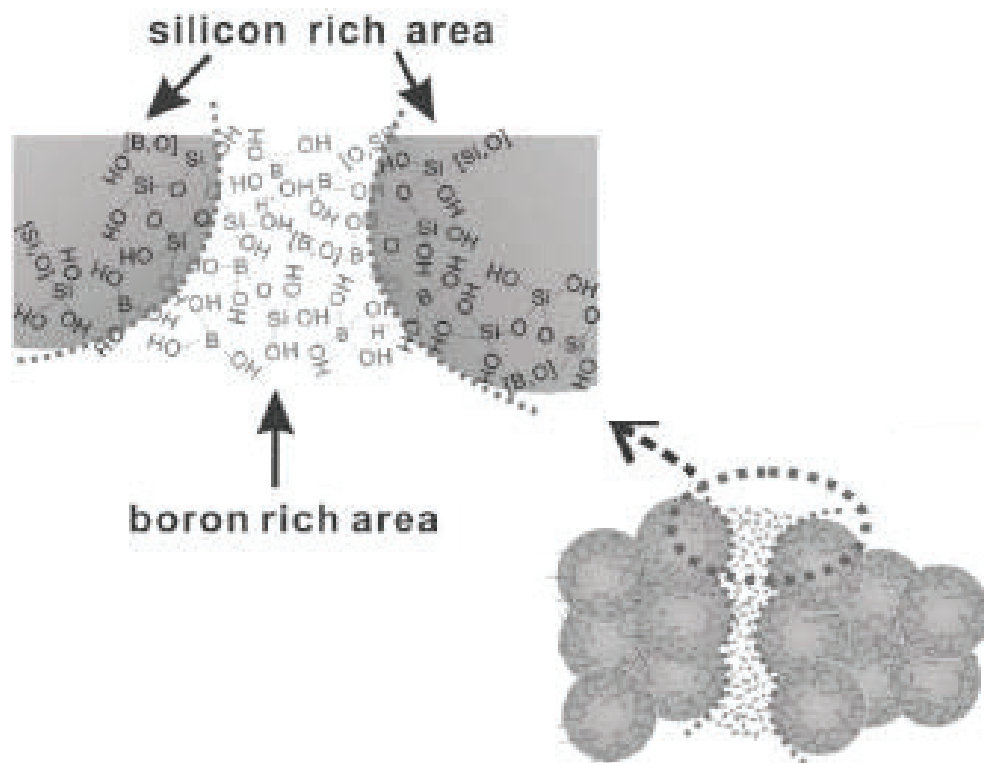


Figure 41 Literature example of easily removed cementing structure  
(Source: Ding et. al., 2017).<sup>46</sup>

#### 4.1.6. Material Balance

In order to obtain a material balance for boron element, ICP, FTIR and XRD analysis were performed using nanoparticles and the supernatants. The ICP results of the supernatants and solid parts are given in *Table 12* and *Table 13*.

First of all, when supernatant was analyzed, it was calculated that the 70% of boron was actually inside the structure. Second, when solid part was analyzed by wet digestion, it was found that nearly 65% of boron was inside the structure of composite nanoparticle and not achievable to hydrolyze or decompose.

Table 12 ICP results of supernatant

B initial (mg)	B supernatant (mg)	B solid (mg)	%
8.700	2.415	6.285	72.241
8.700	2.450	6.250	71.839
8.700	2.580	6.120	70.344

Table 13 ICP results of solid part

B solid (mg)	B supernatant (mg)	B solid (mg)	%
2.146	0.148	1.998	93.103
2.755	0.200	2.555	92.740
2.042	0.142	1.900	93.046

These results were supported by solid particle analyzes before and after water treatment. As seen in FTIR results;  $\text{BO}_3$  peak decreased, SiO peak increased, Si-OH peak appeared and Si-O-Si peak shifted to higher wave numbers (*Figure 42*). In the case of XRD analysis, on the other hand, after treatment, characteristic silica peak dominated the XRD result of composite nanoparticle (*Figure 43*).

Based on these results, it is concluded that:

- ✓ Around 65-70 % of elemental boron was present inside the composite structure
- ✓ The boron is most probably bonded with Si-OH groups situated on the silica surfaces of the composite nanoparticles (*Figure 44*).
- ✓ After the treatment of nanoparticles in water, the characteristic peaks of boron were became weaker and Si-OH peaks were appeared in the spectrum. Also, shift effect became reversed.
- ✓ According to XRD results, amorphous borate peak shifted back towards the amorphous silica peak.

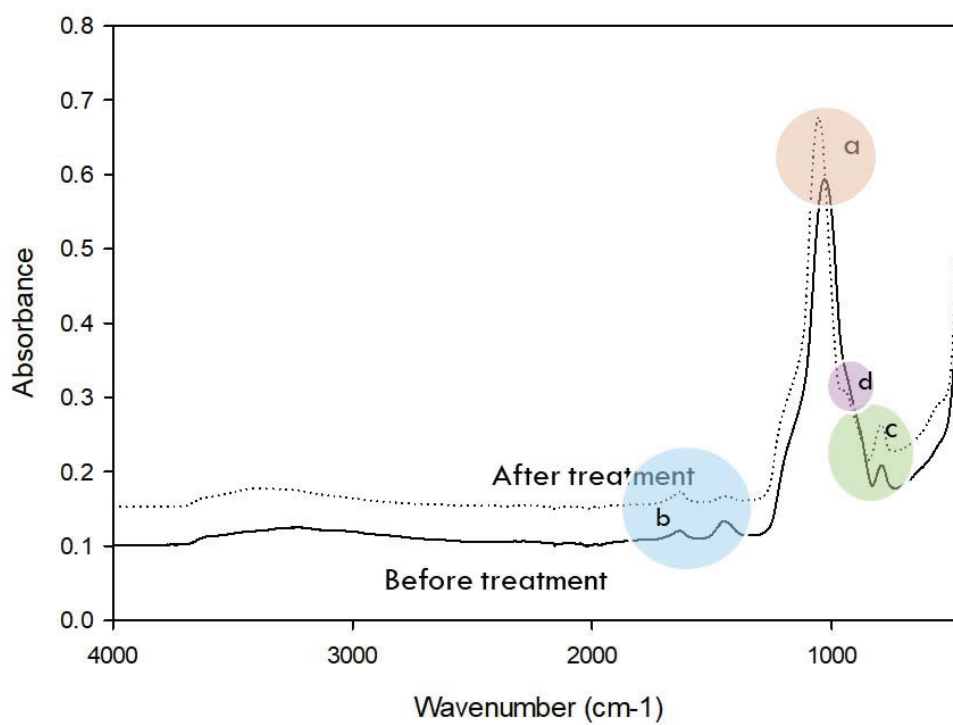


Figure 42 FTIR results of before and after treatment with water.

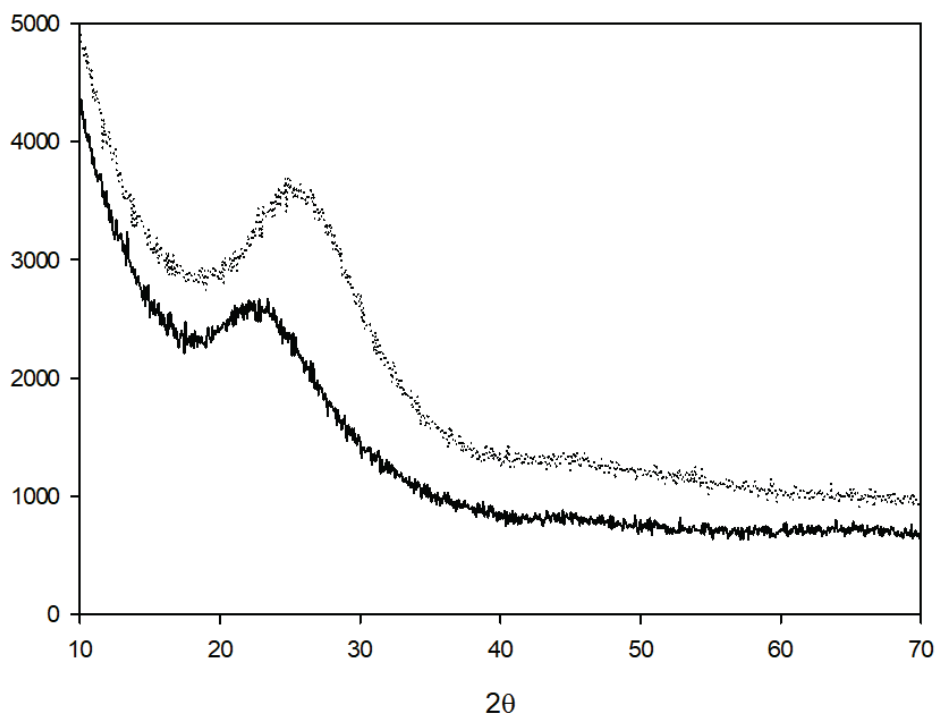


Figure 43 XRD results of before and after treatment with water.

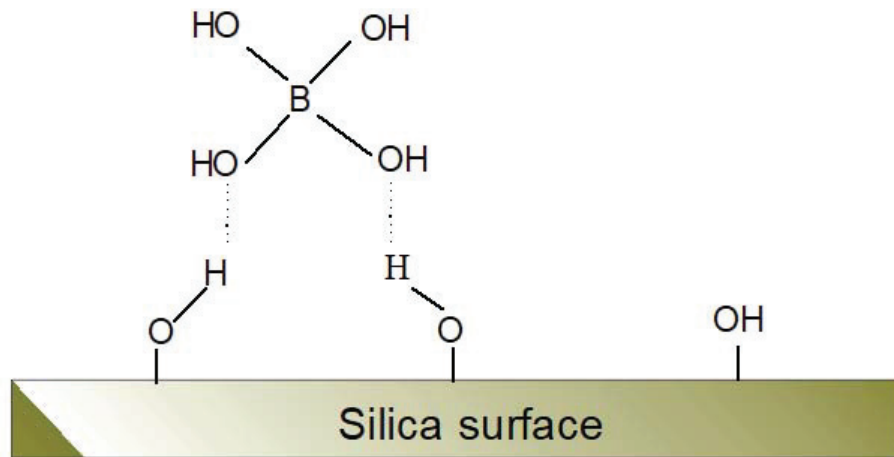


Figure 44 Mechanism of forming composite structure.

## 4.2. Tribological Performance of Composite Nanoparticles

Before performance tests, the Four Ball Tests, nanoparticles that contain 5% Na-Borate were dispersed in different carriers. Then, EP/AW performances of additives tested using Four Ball Test Method according to the standards of ASTM.

### 4.2.1. Dispersion of Composite Nanoparticles in Different Medium

Silica/Na-Borate particles were dispersed in Base Oil 1 with using ultrasonic probe in the presence of CTAB, a cationic surfactant, and the stability of particles were tested after one week later, visually. As seen in *Figure 45* that, there is no phase separation and settlement during this period. That is, the dispersed particles were stable enough for four ball performance tests.

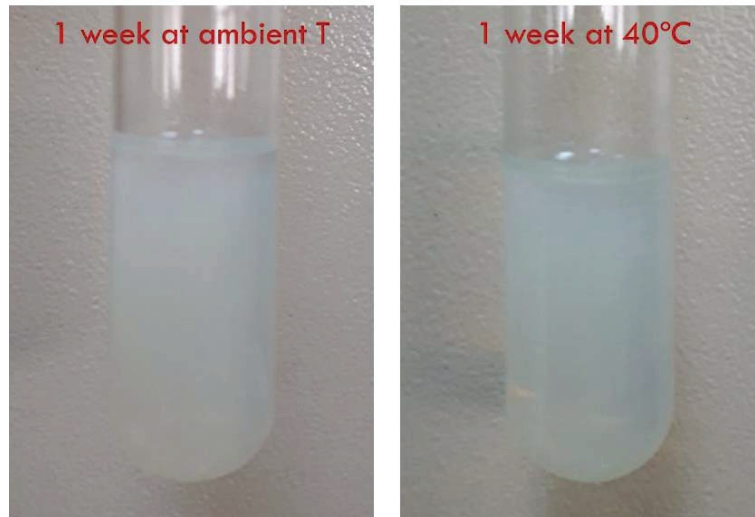


Figure 45 Stability results of composite nanoparticles dispersed in base oil.

#### **4.2.2. Four Ball Extreme Pressure Test and Define the Load-Wear Index and Weld Point**

Lubricants used in moving equipment operating under heavy loads are expected to be resistant to excessive pressure in system and to protect metal surfaces as much as possible without being worn. Lubricant film on metal surface can be destroyed under extreme pressure resulting welding of moving surfaces. With Four Ball EP test, it is aimed to determine load resistance and overpressure characteristics of lubricating oil by simulating this situation.

Our composite nanoparticles dispersed in oils were tested in neat cutting oil formulation by Opet Fuchs. Three different ratio of additives were tested to compare with neat base oil and commercial neat cutting oils. The results of these studies were given in Table 14. As seen from the table (*Table 14*) that, the load carrying capacity of composite nanoparticles were same as commercial additives even if their amounts were five times lower.

Table 14 Four Ball Test - EP performance results of composite nanoparticles

	Commercial Neat-Cutting Oil	Neat Base Oil	Design 1	Design 2	Design 3
Additive Amount (%)	-	-	0.15	0.20	0.30
Welding Load (N)	8000	1000	1260	6200	8000

## CHAPTER 5

### CONCLUSION

It is known that the performance of boron compounds against wear and friction is relatively high when compared to that of conventional lubricant additives. Most of boron compounds, especially boric acid, h-BN and borate derivatives, are used to avoid friction, wear and welding. To date, the foremost challenge for using boron compounds is dispersion and stability. Therefore, the design of easily dispersible, high performance boron-based additives for lubrication is open to development.

In this study, composite nanoparticles were synthesized in nanometer range including both sodium borate and silica. In order to obtain these spherical nanoparticles, Stöber method was modified and used.

It was found that synthesis of composite nanoparticles in desired size distribution and morphology as well as composite structures composed of Si and Na-Borate, was possible by changing the amounts of ingredients and modes of Na-Borate solution addition.

It was concluded that:

- ✓ Composite Silica/Na-Borate nanoparticles were synthesized at a size range of 100 to 900 nm when TEOS was polymerized in the presence of Na-Borate.
- ✓ Gradual addition of Na-Borate co-precipitated with silica in the form of amorphous composite spherical particles. Both the mean size and the distribution of the composite particles varied with the amount of Na-Borate added.
- ✓ Almost all Na-Borate in solution was fixed in the structure of the composite particles up to 5% Na-Borate.
- ✓ At higher borate concentrations or faster addition rates, Na-Borate precipitated as a shell-like phase around the composite particles cementing the individual particles.



- ✓ At even higher borate concentrations or with direct addition, Na-Borate precipitated as a separate phase aside the composite particles.
- ✓ The stability of the composite Silica/Na-Borate nanoparticles was achieved by a cationic surfactant. It can still be improved by use of silane or/and oleic acid based surfactants.
- ✓ The four-ball tests in OPET Fuchs have shown that load carrying capacity of composite nanoparticles were at least same as the commercial additives even if they are used at lower amounts.

## REFERENCES

1. Bhushan, B., *Modern Tribology Handbook, two volume set* ; CRC press, 2000.
2. Li, J. S.; Hao, L. F.; Xu, X. H.; Zhang, L.; Ren, T. H. Preparation, Characterization and Tribological Evaluation of Calcium Borate Nanoparticles as Lubricant Additives. *Advanced Materials Research* **2011**, *148*, 1047-1056.
3. Zhao, G.; Zhao, Q.; Li, W.; Wang, X.; Liu, W. Tribological Properties of Nano-calcium Borate as Lithium Grease Additive. *Lubr. Sci.* **2014**, *26*(1), 43-53.
4. Hao, L.; Li, J.; Xu, X.; Ren, T. Preparation and Tribological Properties of a Kind of Lubricant Containing Calcium Borate Nanoparticles as Additives. *Ind. Lubr. Tribol.* **2012**, *64*(1), 16-22.
5. Hu, Z. S.; Dong, J. X.; Chen, G. X.; He, J. Z. Preparation and Tribological Properties of Nanoparticle Lanthanum Borate. *Wear* **2000**, *243*(1-2), 43-47.
6. Hu, Z. S.; Lai, R.; Lou, F.; Wang, L. G.; Chen, Z. L.; Chen, G. X.; Dong, J. X. Preparation and Tribological Properties of Nanometer Magnesium Borate as Lubricating Oil Additive. *Wear* **2002**, *252*(5-6), 370-374.
7. Hu, Z. S.; Shi, Y. G.; Wang, L. G.; Peng, Y.; Chen, G. X.; Dong, J. X. Study on Antiwear and Reducing Friction Additive of Nanometer Aluminum Borate. *Lubr. Eng.* **2001**, *57*(3), 23-27.
8. Savrik, S. A.; Balkose, D.; Ulku, S. Synthesis of Zinc Borate by Inverse Emulsion Technique for Lubrication. *J. Therm. Anal. Calorim.* **2011**, *104*(2), 605-612.
9. Liu, W. M.; Bing, Z.; Huang, C. X.; Zhang, X. S.; Xue, Q. J.; Wang, H. Q. The Antiwear Properties of Potassium Borate as an Oil Additive. *Lubr. Eng.* **1991**, *47*(5), 344-347.
10. Kong, L. T.; Hu, H.; Wang, T. Y.; Huang, D. H.; Fu, J. J. Synthesis and Surface Modification of the Nanoscale Cerium Borate as Lubricant Additive. *J. Rare. Earth.* **2011**, *29*(11), 1095-1099.
11. Mang, T.; Dresel, W.; *Lubricants and Lubrication*; Wiley-Vch Weinheim, Germany, 2007; Vol. 2.
12. Forces and Newton's Laws of Motion. [http://www.sfu.ca/phys/100/1104/iclicker/04\\_LectureOutlines\\_PRS.pdf](http://www.sfu.ca/phys/100/1104/iclicker/04_LectureOutlines_PRS.pdf). (accessed May 2, 2019).
13. Stick-slip phenomenon. [https://en.wikipedia.org/wiki/Stick-slip\\_phenomenon](https://en.wikipedia.org/wiki/Stick-slip_phenomenon). (accessed May 1, 2019).
14. Kuo, C. H. (Ed.); *Tribology: Lubricants and Lubrication*; InTech: Croatia, 2011.
15. Czichos, H.; *Tribology: A Systems Approach to the Science and Technology of Friction, Lubrication, and Wear*; Elsevier, 2009; Vol 1.

16. *Lubricant Additives: Use and Benefits 2016*; Technical Committee of Petroleum Additive Manufacturers in Europe AISBL (ATC): Brussels, Belgium, 2016.
17. Bhushan, B.; *Introduction to Tribology, 2<sup>nd</sup> Edition*; John Wiley & Sons, 2013: United Kingdom.
18. *White Paper-Additive Glossary 2018*; Exxon Mobile Corporation: Texas, USA.
19. Shah, F. U. Boron Compounds as Additives to Lubricants: Synthesis, Characterization and Tribological Optimization. Ph.D. Thesis, Lulea Tekniska Universitet, 2009.
20. Antiwear additive. [https://en.wikipedia.org/wiki/Antiwear\\_additive](https://en.wikipedia.org/wiki/Antiwear_additive). (accessed May 15, 2019).
21. Gegner, J. (Ed.); *Tribology: Fundamentals and Advancements*; BoD–Books on Demand, 2013.
22. Extreme pressure additive. [https://en.wikipedia.org/wiki/Extreme\\_pressure\\_additive](https://en.wikipedia.org/wiki/Extreme_pressure_additive). (accessed May 7, 2019).
23. Shah, F. U.; Glavatskih, S.; Antzutkin, O. N. Boron in Tribology: From Borates to Ionic Liquids. *Tribol. Lett.* **2013**, *51*(3), 281-301.
24. Dresel, W.; Mang, T.; *Lubricants and Lubrication. 2<sup>nd</sup> ed.*; Weinheim, Germany: Wiley-Vch., 2017.
25. David W. Johnson, J. E. H. Phosphate Esters, Thiophosphate Esters and Metal Thiophosphates as Lubricant Additives. *Lubricants* **2013**, *1*, 132-148.
26. Shahnazar, S.; Bagheri, S.; Abd Hamid, S. B. Enhancing Lubricant Properties by Nanoparticle Additives. *International Journal of Hydrogen Energy* **2016**, *41*(4), 3153-3170.
27. Limitations of Extreme Pressure Additives. <https://www.machinerylubrication.com/Read/29031/extreme-pressure-additives>. (accessed April 24, 2019).
28. Dai, W.; Kheireddin, B.; Gao, H.; Liang, H. Roles of Nanoparticles in Oil Lubrication. *Tribol. Int.* **2016**, *102*, 88-98.
29. Gulzar, M.; Masjuki, H. H.; Kalam, M. A.; Varman, M.; Zulkifli, N. W. M.; Mufti, R. A.; Zahid, R. Tribological Performance of Nanoparticles as Lubricating Oil Additives. *Journal of Nanoparticle Research* **2016**, *18*(8), 223.
30. Zeng, Y.; Yang, H.; Fu, W.; Qiao, L.; Chang, L.; Chen, J.; Zhu, H.; Li, M.; Zou, G. Synthesis of Magnesium Borate (Mg<sub>2</sub>B<sub>2</sub>O<sub>5</sub>) Nanowires, Growth Mechanism and Their Lubricating Properties. *Mater. Res. Bull.* **2008**, *43*(8-9), 2239-2247.
31. Chen, G.; Hu, Z.; Nai, R.; Wang, L.; Peng, Y.; Dong, J. Preparation and Tribology of Ultrafine and Amorphous Strontium Borate. *Proceedings of the Institution of Mechanical Engineers, Part L: Journal of Materials: Design and Applications* **2001**, *215*(3), 133-140.

32. Dong, J.; Hu, Z. A Study of The Anti-Wear and Friction-Reducing Properties of the Lubricant Additive, Nanometer Zinc Borate. *Tribol. Int.* **1998**, *31*(5), 219-223.
33. Tian, Y.; Guo, Y.; Jiang, M.; Sheng, Y.; Hari, B.; Zhang, G.; Jiang, Y.; Zhou, B.; Zhu, Y.; Wang, Z. Synthesis of Hydrophobic Zinc Borate Nanodiscs for Lubrication. *Mater. Lett.* **2006**, *60*(20), 2511-2515.
34. Hu, Z.; Dong, J. Study on Antiwear and Reducing Friction Additive of Nanometer Titanium Borate. *Wear* **1998**, *216*(1), 87-91.
35. Baş, H.; Karabacak, Y. E. Investigation of the Effects of Boron Additives on the Performance of Engine Oil. *Tribol. T.* **2014**, *57*(4), 740-748.
36. López, T. D.-F.; González, A. F.; Del Reguero, Á.; Matos, M.; Díaz-García, M. E.; Badía-Laiño, R. Engineered Silica Nanoparticles as Additives in Lubricant Oils. *Science and Technology of Advanced Materials* **2015**, *16*(5), 055005.
37. Sui, T.; Song, B.; Zhang, F.; Yang, Q. Effect of Particle Size and Ligand on the Tribological Properties of Amino Functionalized Hairy Silica Nanoparticles as an Additive to Polyalphaolefin. *J. Nanomater.* **2015**, *16*(1), 427.
38. Stöber, W.; Fink, A.; Bohn, E. Controlled Growth of Monodisperse Silica Spheres in the Micron Size Range. *Journal of Colloid and Interface Science* **1968**, *26*(1), 62-69.
39. Green, D. L.; Jayasundara, S.; Lam, Y.-F.; Harris, M. T. Chemical Reaction Kinetics Leading to the First Stober Silica Nanoparticles – NMR and SAXS Investigation. *J. Non-Cryst. Solids* **2003**, *315*(1–2), 166-179.
40. Stöber Process. [https://en.wikipedia.org/wiki/St%C3%B6ber\\_process](https://en.wikipedia.org/wiki/St%C3%B6ber_process). (accessed June 21, 2019).
41. Four Ball Tester. <https://koehlerinstrument.com/products/four-ball-tester/>. (accessed May 30, 2019).
42. Weld Load by Shell Four-Ball Test [https://www.sumico.co.jp/e/qa/qa\\_t\\_shell\\_e.html](https://www.sumico.co.jp/e/qa/qa_t_shell_e.html). (accessed May 30, 2019).
43. Four Ball Tester - Extreme Pressure (EP) Test. <https://ducom.com/test-instruments/lubricant-testers/four-ball-tester/>. (accessed May 30, 2019).
44. Theiss, F. L.; Ayoko, G. A.; Frost, R. L. Removal of Boron Species by Layered Double Hydroxides: A Review. *J. Colloid Interface Sci.* **2013**, *402*, 114-21.
45. Geng, S.; Shah, F. U.; Liu, P.; Antzutkin, O. N.; Oksman, K. Plasticizing and Crosslinking Effects of Borate Additives on the Structure and Properties of Poly(vinyl acetate). *Rsc. Adv.* **2017**, *7*(13), 7483-7491.
46. Ding, S.; Liu, N.; Li, X.; Peng, L.; Guo, X.; Ding, W. Silica Nanotubes and Their Assembly Assisted by Boric Acid to Hierarchical Mesostructures. *Langmuir* **2010**, *26*(7), 4572-5.